Accepted Manuscript

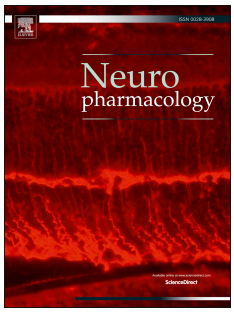

Lethal effects of an insecticidal spider venom peptide involve positive allosteric modulation of insect nicotinic acetylcholine receptors

Monique J. Windley, Irina Vetter, Richard J. Lewis, Graham M. Nicholson

PII: S0028-3908(17)30149-1

DOI: 10.1016/j.neuropharm.2017.04.008

Reference: NP 6664

To appear in: *Neuropharmacology*

Received Date: 23 January 2017

Revised Date: 28 March 2017

Accepted Date: 6 April 2017

Please cite this article as: Windley, M.J., Vetter, I., Lewis, R.J., Nicholson, G.M., Lethal effects of an insecticidal spider venom peptide involve positive allosteric modulation of insect nicotinic acetylcholine receptors, *Neuropharmacology* (2017), doi: 10.1016/j.neuropharm.2017.04.008.

Submitted to *Neuropharmacology*

Lethal effects of an insecticidal spider venom peptide involve positive allosteric modulation of insect nicotinic acetylcholine receptors

Monique J. Windley[a], Irina Vetter[b,c], Richard J. Lewis[b], Graham M. Nicholson[a,*]

[a] *School of Life Sciences, University of Technology Sydney, P.O. Box 123, Broadway NSW 2007, Australia;*

[b] *Institute for Molecular Bioscience, University of Queensland, Brisbane, Australia*

[c] *School of Pharmacy, University of Queensland, Brisbane, Australia*

* Corresponding author. Prof Graham M. Nicholson, Faculty of Science, University of Technology Sydney, P.O. Box 123, Broadway NSW 2007, Australia.

Email address: Graham.Nicholson@uts.edu.au (G.M. Nicholson).

TEL [61-2] 9514 2230, FAX [61-2] 9514 1656

Highlights

- The previously characterized BK_{Ca} channel block is not responsible for the lethal excitatory toxicity of κ-HXTX-Hv1c
- κ-HXTX-Hv1c is a positive allosteric modulator of the insect nicotinic acetylcholine receptor which acts by prolonging current decay and reversing receptor desensitization
- The likely lethal target of κ-HXTX-Hv1c is the nicotinic acetylcholine receptor, acting by a mechanism similar to that of the insecticide spinosyn A.

A B S T R A C T

κ-Hexatoxins (κ-HXTXs) are a family of excitotoxic insect-selective neurotoxins from Australian funnel-web spiders that are lethal to a wide range of insects, but display no toxicity towards vertebrates. The prototypic κ-HXTX-Hv1c selectively blocks native and expressed cockroach large-conductance calcium-activated potassium (BK_{Ca} or $K_{Ca}1.1$) channels, but not their mammalian orthologs. Despite this potent and selective action on insect $K_{Ca}1.1$ channels, we found that the classical $K_{Ca}1.1$ blockers paxilline, charybdotoxin and iberiotoxin, which all block insect $K_{Ca}1.1$ channels, are not lethal in crickets. We therefore used whole-cell patch-clamp analysis of cockroach dorsal unpaired median (DUM) neurons to study the effects of κ-HXTX-Hv1c on sodium-activated (K_{Na}), delayed-rectifier (K_{DR}) and 'A-type' transient (K_A) K^+ channels. 1 μM κ-HXTX-Hv1c failed to significantly inhibit cockroach K_{Na} and K_{DR} channels, but did cause a 30 ± 7% saturating inhibition of K_A channel currents, possibly via a Kv4 (Shal-like) action. However, this modest action at such a high concentration of κ-HXTX-Hv1c would indicate a different lethal target. Accordingly, we assessed the actions of κ-HXTX-Hv1c on neurotransmitter-gated ion channels in cockroach DUM neurons. We found that κ-HXTX-Hv1c failed to produce any major effects on $GABA_A$ or glutamate-Cl receptors but dramatically slowed nicotine-evoked ACh receptor (nAChR) current decay and reversed nAChR desensitization. These actions occurred without any alterations to nAChR current amplitude or the nicotine concentration-response curve, and are consistent with a positive allosteric modulation of nAChRs. κ-HXTX-Hv1c therefore represents the first venom peptide that selectively modulates insect nAChRs with a mode of action similar to the excitotoxic insecticide spinosyn A.

Keywords: Spider toxins, bioinsecticide, nAChR PAM, insect-selective, peptide toxins

Abbreviations: 4-AP, 4-aminopyridine; $K_{Ca}1.1$ channel, large-conductance Ca^{2+} and voltage-gated K^+ channel (also known as Maxi-K, BK, or Slo1); Ca_V channel, voltage-gated Ca^{2+} channel; ChTx, charybdotoxin (potassium channel scorpion toxin α-KTx1.1); DUM, dorsal unpaired median; HXTX, hexatoxin (from the venom of spiders belonging to the family Hexathelidae); IbTx, iberiotoxin (potassium channel scorpion toxin α-KTx1.3); $I_{K(A)}$, transient A-type K^+ current; $I_{BK(Ca)}$, calcium-

activated K^+ channel current; $I_{K(DR)}$, delayed-rectifier K^+ current; α-KTx, potassium channel scorpion toxin; K_A channel, 'A-type' transient K^+ channel; KD_{50}, median knockdown dose; K_{DR} channel, delayed-rectifier K^+ channel; K_{Na} channel, sodium-activated K^+ channel; K_V channel, voltage-gated K^+ channel; nAChR, nicotinic acetylcholine receptor; mSlo, mouse slowpoke channel; Na_V channel, voltage-gated sodium channel; NIS, normal insect saline; pSlo, *Periplaneta* slowpoke channel; κ-SPRTX-Hv1b, κ-sparatoxin-Hv1b (formerly heteropodotoxin-2 from the venom of *Heteropoda venatoria*, family Sparassidae); TAG, terminal abdominal ganglion; TEA, tetraethylammonium; κ-TRTX-Ps1a, κ-theraphotoxin-Ps1a (formerly phrixotoxin-1 from the venom of *Paraphysa scrofa*, family Theraphosidae), TTX, tetrodotoxin.

Funding

Financial support for this study was provided by an Australian Postgraduate Award to M.J.W.

1. Introduction

As insects continue to develop resistance against current agrochemical insecticides, it is critical to source a new pool of insect-selective lead molecules with novel targets. Spider venoms are a relatively untapped source of potentially millions of insecticidal peptide toxins including the excitatory neurotoxin κ-HXTX-Hv1c (See Windley et al., 2012 for a review). Isolated from the venom of the Blue Mountains funnel-web spider, *Hadronyche versuta* (Hexathelidae: Atracinae), κ-HXTX-Hv1c is lethal against a number of agriculturally and medically important arthropod pests (Maggio and King, 2002a; Tedford et al., 2007; Wang et al., 2000), however it lacks overt toxicity against a number of vertebrates including mice, rabbits, rats and chickens (Wang et al., 2000).

Whole-cell patch-clamp studies on American cockroach (*Periplaneta americana*) dorsal unpaired median (DUM) neurons revealed that κ-HXTX-Hv1c selectively targets voltage-gated potassium currents (I_K) (Gunning et al., 2008). The selective inhibition of the global I_K is a result of potent block of large-conductance calcium-activated potassium ($K_{Ca}1.1$) channel currents (IC_{50} of 2 and 240 nM for native and expressed channels, respectively), and a minor inhibition of K_A channel currents (Gunning et al., 2008). Block of $K_{Ca}1.1$ was found to be insect-selective, confirmed by a lack of activity on native rat dorsal root ganglion, and heterologously expressed mouse (mSlo) $K_{Ca}1.1$ channels.

Despite the potent and, seemingly, selective actions of κ-HXTX-Hv1c on insect $K_{Ca}1.1$ channels, this fails to conclusively demonstrate that $K_{Ca}1.1$ channels are the lethal target in insects. Although evidence indicates that the pharmacophores for block of $K_{Ca}1.1$ channels and insect lethality are almost identical (Gunning et al., 2008), it cannot be ruled out that the same, or overlapping, residues are responsible for toxin interactions with additional targets that remain unexplored. The evidence that brings into question whether the $K_{Ca}1.1$ channel is the prime insecticidal target arises from the finding

that genetic mutations that eliminate I_{KCa} do not appear to be lethal in *Drosophila* (Elkins et al., 1986). In addition, there are several other neurological ion channel targets that merit further investigation.

There are range of insect voltage- and neurotransmitter-gated receptors that represent potential candidates for the lethal activity of κ-HXTX-Hv1c. The prospective voltage-gated ion channel targets include the transient potassium current (Gunning et al., 2008) and the, yet untested, sodium-gated potassium channel; while neurotransmitter-gated contenders include the excitatory nicotinic-gated acetylcholine receptor (nAChR) or the inhibitory glutamate- (GluCl) and GABA-gated (GABA-Cl) chloride receptors. Receptor subtypes within these neurotransmitter families are not well characterized in insects, however studies suggest that at least two subtypes exist for each receptor based on pharmacological and kinetic profiles. GABA subtypes are distinguished by dieldrin, fipronil and picrotoxinin block (Le Corronc et al., 2002), GluCl by sensitivity to fipronil and the presence of desensitization (Narahashi et al., 2010) and nAChR by sensitivity to α-bungarotoxin (α-BgTx). Investigations on cockroach neurons have revealed that α-BgTx sensitive nAChR receptors may even be dissected further based on mixed nicotine, muscarinic activity with slow or fast current decay (Lapied et al., 1990), and sensitivity to spinosyn A (Salgado and Saar, 2004), while α-BgTx resistant receptor subtypes are defined by sensitivity to *d*-tubocurarine (AChR1 and nAChR2) (Courjaret and Lapied, 2001).

The initial aim of this study was to determine if $K_{Ca}1.1$ channels are viable insecticide targets. Considering the absence of lethal effects following block of insect K_V channels, the subsequent aim of this study was to determine additional targets capable of mediating the lethal effects of κ-HXTX-Hv1c in insects. The present study found that there were no significant effects of κ-HXTX-Hv1c on $GABA_AR$, and only minor effects on GluClR currents, however, it was found that κ-HXTX-Hv1c caused a potent concentration-dependent positive allosteric modulation of nAChR. This was associated with a prolongation of the decay of nicotine-evoked currents and the reversal of nAChR desensitization. As the nAChR is already a known target of insecticides this receptor is the most likely candidate for the lethal excitatory activity of κ-HXTX-Hv1c.

2. Materials and methods

2.1. Acute toxicity testing

The insecticidal activity of several K_V channel blockers was assessed in unsexed 3^{rd}–4^{th} instar juvenile house crickets (*Acheta domesticus*; Pisces Enterprises Pty. Ltd., Kenmore, Queensland). Crickets of mass 80–120 mg were injected intrathoracically with 2–6 µl of solution using a 0.5 ml precision syringe. An Arnold microapplicator (Burkhard Scientific Supply, Rickmansworth, England) was used to inject toxin into the upper dorsal region of the thorax, between the second and third pair of

legs, using a 29-gauge syringe. Purified toxins were dissolved in normal insect saline (NIS) containing (in mM): NaCl 200, KCl 3.1, $CaCl_2$ 5.4, $MgCl_2$ 4, $NaHCO_3$ 2, Na_2HPO_4 0.1 with the addition of 0.1% bovine albumin serum (BSA) to reduce non-specific binding, and the pH adjusted to 7.4 with 1 M NaOH. Concentrated toxin solutions were made up in > 90% NIS. In addition, paxilline was dissolved in 0.7% v/v ethanol in insect saline. Control experiments indicated that the presence of 0.7% v/v ethanol did not cause any overt signs of acute toxicity in crickets.

Between 10 and 30 crickets were injected at each toxin concentration with 5 µl/100 mg bodyweight, while a control group of 10 crickets were injected with insect saline/0.1% BSA. Percentage lethality was noted at 12, 24, 48 and 72 h following injection. Knockdown, defined as the loss of the righting reflex or the inability to remain upright, was also recorded at the same time points. Median knockdown (KD_{50}) and lethal (LD_{50}) doses were calculated from data fitted by a Logistic equation (See Eq. 2).

2.2. Isolation of insect neurons

The whole-cell patch-clamp technique was employed to identify the lethal target(s) of κ-HXTX-Hv1c in the insect nervous system (Hamill et al., 1981). Dorsal unpaired median (DUM) neurons were used in this study, as they are the most comprehensively characterized neurons in the insect nervous system. They generate spontaneous action potentials and contain a range on voltage-gated and neurotransmitter-gated ion channels known to play fundamental roles in the insect nervous system (Grolleau and Lapied, 2000; Wicher et al., 2001). Furthermore, they contain all the ion channels groups targeted by insecticides to date and as such are a useful model for the purpose of this study.

DUM neurons, isolated from the terminal abdominal ganglion (TAG) of unsexed American cockroaches (*Periplaneta americana*), were used for all patch-clamp experiments in this study (Gunning et al., 2008; Lapied et al., 1989; Windley et al., 2011). Single adult DUM neurons were isolated from cockroach TAG through mechanical and enzymatic dissociation, as previously described (Gunning et al., 2008; Windley et al., 2011). Briefly, TAG were dissected from the ventral nerve cord and transferred to Ca^{2+}/Mg^{2+}-free NIS containing (in mM): NaCl 180, KCl 3.1, N-hydroxyethylpiperazine-N-ethanesulfonic acid (HEPES) 10 and D-glucose 20. Following the mechanical removal of the external sheath, TAG were incubated in 1 mg/ml collagenase (type IA) dissolved in NIS for 40 min at 29 °C. Ganglia were washed and resuspended in NIS supplemented with 5% fetal bovine serum (FBS) and 0.1% penicillin/streptomycin. Individual neurons were dissociated by gentle trituration of ganglia through a lightly fire-polished Pasteur pipette. Dissociated neurons were dispensed onto 12-mm diameter glass coverslips pre-coated with 1 mg/ml concanavalin A (type IV) and maintained in NIS supplemented with 5% FBS and 0.1% penicillin/streptomycin at 30 °C, 100% humidity for no longer than 24 h.

2.3. Whole-cell patch-clamp electrophysiology

Ion channel currents and action potentials were evoked in voltage-clamp and current-clamp mode, respectively. Data were recorded using the pCLAMP (versions 9 and 10) data acquisition system (Molecular Devices, Sunnyvale, CA, USA) and filtered at 5 kHz with a low-pass Bessel filter. Leakage and capacitive currents were subtracted using *P-P*/4 procedures. Digital sampling rates were between 15 and 25 kHz for voltage-gated ion channel recordings and 2 kHz for transmitter-gated ion channel recordings. Single-use electrodes were pulled from borosilicate glass with d.c. resistances of *ca*. 1, 1.5 and 2.5 MΩ for Na_V, Ca_V and K_V channel current recordings, respectively, and 1–2 MΩ for glutamate-, GABA- and nicotinic acetylcholine-gated (nACh) channel current recordings. Liquid junction potentials for the various combinations of internal pipette and external bath solutions were calculated using JPCALC (Barry, 1994), and all data were compensated for these values. Series resistance compensation was >80% for all cells. Cells were bathed in external solution through a continuous pressurized perfusion system at 1 ml/min, while toxin and receptor agonist solutions were introduced via direct pressurized application via a perfusion needle at *ca*. 50 µl/min/psi (Automate Scientific, San Francisco, CA). All experiments were performed at ambient room temperature (20–23 °C).

2.3.1. Action potential recordings

Cockroach DUM neurons are spontaneously active and at resting membrane potentials most are capable of generating repetitive overshooting action potentials with firing frequencies of around 6–7 Hz (Grolleau and Lapied, 2000). To record spontaneous action potentials under current-clamp conditions the external solution contained (in mM): NaCl 190, KCl 3.1, $CaCl_2$ 5, $MgCl_2$ 4 and HEPES 10. The pH was adjusted to 7.4 with 1 M NaOH. Internal pipette solutions for recording action potentials included (in mM): K gluconate 160, KF 10, $CaCl_2$ 0.5, NaCl 15, $MgCl_2$ 1, HEPES 10 and EGTA 10. The pH was adjusted to 7.4 with 2 M KOH and the osmolarity of both internal and external solutions was adjusted to 400 ± 5 mOsmol/L with sucrose. In order to record spontaneous action potentials, gap-free recordings for 5 s were made at 1-min intervals in the absence of current stimuli.

2.3.2. Voltage-gated ion channel electrophysiology

To record the effects of **κ**-HXTX-Hv1c on isolated voltage- and neurotransmitter-gated ion channels a number of voltage-clamp protocols, different bathing and pipette solutions, as well ion channel blockers, were used.

The external bath solution for recording all DUM neuron $I_{K,}$ apart from $I_{K(Na)}$, contained (in mM): NaCl 150, KCl 30, $CaCl_2$ 5, $MgCl_2$ 4, TTX 0.3, HEPES 10 and D-glucose 10. The pipette solution consisted of (in mM): KCl 135, KF 25, NaCl 9, $CaCl_2$ 0.1, $MgCl_2$ 1, EGTA 1, HEPES 10 and ATP-Na_2 3.

To record outward $I_{K(DR)}$ in DUM neurons, $I_{K(A)}$ were blocked by the addition of 5 mM 4-aminopyridine (4-AP) to the external solution (Grolleau and Lapied, 1995; Gunning et al., 2008;

Windley et al., 2011). $I_{K(Na)}$ and voltage-gated Na^+ channel currents (I_{Na}) were blocked by the addition of 300 nM TTX to the external solution, while $K_{Ca}1.1$ channels were blocked by the combination of 30 nM IbTx and 1 mM $CdCl_2$ that also blocked voltage-gated Ca^{2+} (Ca_V) channels.

$K_{Ca}1.1$ channel currents ($I_{BK(Ca)}$) could not be recorded in isolation from $I_{K(DR)}$ because there are no selective blockers of insect $I_{K(DR)}$. Consequently, $K_{Ca}1.1$ channel current isolation was achieved using the following procedure (Gunning et al., 2008; Windley et al., 2011). Initially, both $I_{K(DR)}$ and $I_{K(Ca)}$ were recorded concurrently (protocol 1). Secondly, the test compound was applied and whole-cell currents were recorded until equilibrium was reached (typically 5 min of perfusion; protocol 2). Finally, 100 nM IbTx was perfused to completely eliminate $I_{BK(Ca)}$ (protocol 3). The subsequent isolation of $I_{K(Ca)}$ was achieved by offline subtraction of the remaining $I_{K(DR)}$. Thus: $I_{BK(Ca)}$ control = protocol 1 – protocol 3; while $I_{BK(Ca)}$ toxin = protocol 2 – protocol 3. 1 mM $CdCl_2$ and 5 mM 4-AP were included in the external solutions to block Ca_V channel currents and $I_{K(A)}$, respectively (Grolleau and Lapied, 1995; Gunning et al., 2008; Windley et al., 2011). Test pulses to +30 mV for 100 ms from a holding potential (V_h) –80 mV delivered at 0.1 Hz were used to evoke outward non-inactivating K_{DR} and $K_{Ca}1.1$ channel currents. To determine the voltage-dependence of channel activation, families of I_K were evoked by 100-ms depolarizing test pulses from –80 to +60 mV in 10-mV increments, at 0.1 Hz.

To record transient $I_{K(A)}$, 1 mM $CdCl_2$ and 30 nM IbTx were introduced in the external solution to block $K_{Ca}1.1$ channel currents. Furthermore, the $[K^+]_{ext}$ was reduced from 30 mM to 7 mM KCl in order to increase the K^+ driving force and obtain larger $I_{K(A)}$. As with $I_{BK(Ca)}$, $I_{K(A)}$ cannot be recorded in isolation from $I_{K(DR)}$ due to the lack of selective blockers of insect $I_{K(DR)}$. Therefore, $I_{K(A)}$ were isolated from $I_{K(DR)}$ using voltage protocols designed to exploit the inactivation of $I_{K(A)}$ by depolarizing prepulses (Grolleau and Lapied, 1995). Initially, both $I_{K(A)}$ and $I_{K(DR)}$ were elicited by a 100-ms depolarizing test pulse to +40 mV preceded by a 1-s prepulse potential to –100 mV (protocol 1). On every alternate pulse, $I_{K(DR)}$ were recorded in isolation by changing the 1-s prepulse to –20 mV to inactivate $I_{K(A)}$ (protocol 2). In order to isolate $I_{K(A)}$, the currents resulting from protocol 2 ($I_{K(DR)}$) were digitally subtracted offline from the currents resulting from protocol 1 ($I_{K(DR)}$ + $I_{K(A)}$) (see Fig. 1G). Pulse protocols were delivered at 0.33 Hz.

Families of $I_{K(A)}$ and $I_{K(DR)}$ were evoked to assess the voltage dependence of any toxin actions. Test pulses of 100-ms duration from –80 to +60 mV in 10-mV increments, preceded by a 1-s –100 mV (protocol 1) or –20 mV (protocol 2) prepulse, were used to evoke $I_{K(DR)}$ and $I_{K(A)}$ or $I_{K(DR)}$, respectively. In order to isolate $I_{K(A)}$ families, currents resulting from protocol 2 were subtracted offline from those evoked by protocol 1. To record outward transient sodium-activated K_V channel currents ($I_{K(Na)}$), recording solutions adapted from Grolleau and Lapied (1994) were utilized. External solutions contained (in mM): NaCl 100, Tris-Cl 70, KCl 3.1, $CaCl_2$ 1.8, $MgCl_2$ 4, HEPES 10, $CdCl_2$ 1, and 30 nM IbTx, adjusted to pH 7.4 with 1 M NaOH. Neither 4-AP nor TTX were included in the external solution as they both block $I_{K(Na)}$. The pipette solution contained (in mM): KCl 135, KF 25, NaCl 9, $CaCl_2$ 0.1, $MgCl_2$ 1, HEPES 10, EGTA 1 and ATP-Na_2 3, adjusted to pH 7.4 with 2 M KOH. To

isolate $I_{K(Na)}$, channel currents were initially recorded in the absence of TTX. The outward $I_{K(Na)}$ is activated by Na^+ and as such channel activation is closely correlated with the inward Na_V current and subsequently both are blocked by TTX (Grolleau and Lapied, 1994). To record $I_{K(Na)}$ in isolation a similar technique to $I_{K(Ca)}$ isolation was employed. Initially, $I_{K(Na)}$ and I_{Na} were recorded concurrently (protocol 1). Secondly, the test substance was applied and recordings were made until equilibrium was reached (protocol 2). Finally, 300 nM TTX was added in order to block $I_{K(Na)}$ and I_{Na} (protocol 3). Subsequently, through employing offline subtraction of currents evoked by protocol 3 from both protocol 1 and protocol 2, the portion of the outward current sensitive to TTX could be identified. Unfortunately, $I_{K(Na)}$ could not be recorded in isolation from $I_{K(A)}$ as the only characterized blocker of K_A channels, 4-AP additionally inhibits K_{Na} channels (data not shown). As $I_{K(Na)}$ were evoked by test pulses to –10 mV from a holding potential of –90 mV, the contribution of $I_{K(A)}$ would be minimal but still significant enough to take into consideration.

2.3.3. Neurotransmitter-gated ion channel electrophysiology

The effects of κ-HXTX-Hv1c were also assessed on Glu-Cl, GABA-Cl and nACh receptors in DUM neurons. To record whole-cell inward glutamate-gated ($I_{Glu\text{-}Cl}$) and GABA-gated ($I_{GABA\text{-}Cl}$) chloride channel currents the external bath solution consisted of (in mM): NaCl 167, K gluconate 33, KCl 3.1, $MgCl_2$ 4, $CaCl_2$ 5, HEPES 10, pH adjusted with 1 M NaOH. The internal pipette solution contained (in mM): NaCl 15, KCl 170, $MgCl_2$ 1, $CaCl_2$ 0.5, EGTA 10, HEPES 20, phosphocreatine-diTris 10 and 3 ATP-Mg_2, pH adjusted with 2 M KOH.

To record nAChR channel currents (I_{nAChR}) the external bath solution included (in mM): NaCl 200, KCl 3.1, $CaCl_2$ 5, $MgCl_2$ 4, HEPES 10 and 300 nM TTX, pH adjusted to 7.4 with 1 M NaOH. The internal pipette solution contained (in mM): NaCl 10, KCl 170, $CaCl_2$ 0.5, $MgCl_2$ 1, HEPES 20, EGTA 10, ATP-Mg_2 3, pH adjusted with 2 M KOH.

$I_{Glu\text{-}Cl}$, $I_{GABA\text{-}Cl}$ and I_{nAChR} were activated by their cognate neurotransmitters delivered through a pressurized Picospritzer system (Parker, Castle Hill, Australia). Solutions under pressure (2–5 psi) were introduced through a glass micropipette (resistance <0.5 MΩ when filled with agonist) positioned within 50 μm of the DUM neuron. This system allowed for controlled and direct application of agonist while minimizing channel desensitization. With a constant bath flow of 1 ml/min the agonist was rapidly removed from the vicinity surrounding the cell. In no experiment did the pressurized injection of the bath solution with the same protocol result in any deviation from the baseline current.

To establish an agonist dose-response relationship for neurotransmitter-gated ion channels pCLAMP digital inputs were employed to program agonist pulse protocols of varying durations. Assuming a constant pressure is applied, the pulse duration has been shown to be proportional to the log[agonist] value at any point on the cell membrane (McCaman et al., 1977). To confirm that the volume of solution delivered and the pulse duration employed were directly proportional, droplets of solution were injected into a droplet of immersion oil for a known duration and the change in oil

droplet diameter was calculated as an indirect measurement of volume (data not shown). This approach has been employed in a number of previous studies with insect neurons (Courjaret et al., 2003; Lapied et al., 1990). To determine if κ-HXTX-Hv1c alters the sensitivity of transmitter-gated channels to glutamate, GABA or nicotine, dose-response curves were generated from agonist applications ranging from 2.5–1520 ms for $I_{Glu\text{-}Cl}$, 100–1600 ms for $I_{GABA\text{-}Cl}$ and 4–33 ms for I_{nAChR}. Inward currents were evoked at 1-min intervals and gap-free recordings of up to 10 s duration were recorded at –50 mV.

The voltage-dependence of the effect of **κ**-HXTX-Hv1c on $I_{Glu\text{-}Cl}$, $I_{GABA\text{-}Cl}$ and I_{nAChR} were determined in response to 10 ms, 400 ms and 10 ms pulses of agonist, respectively. The membrane voltage was stepped in 10-mV intervals from –70 to +70 mV for durations of 16.25 s from a holding potential of –50 mV for $I_{Glu\text{-}Cl}$ and $I_{GABA\text{-}Cl}$ or 20-mV intervals from –90 to +30 mV from a holding potential of –50 mV for I_{nAChR}. Agonist pulses were applied 3.75 s into the voltage step to allow voltage gated currents to reach steady state and currents were allowed to resolve before stepping back to the holding potential. The membrane potential was held at –50 mV between pulses and during the first and last 5 ms of the pulse protocol. Currents were evoked at 1-min intervals.

In order to assess the ability of a toxin to reverse nAChR desensitization to nicotine, 5-min nicotine pulses were applied at low pressure (2–3 psi) via the Picospritzer pressure ejection system. The toxin was applied 100 s into the nicotine pulse, when channels were partially or fully sensitized. Nicotine delivery was ceased prior to the removal of **κ**-HXTX-Hv1c.

2.4. SH-SY5Y cell culture

SH-SY5Y human neuroblastoma cells were maintained in RPMI medium (ThermoFisher Scientific, Scoresby, Australia) supplemented with 15% foetal bovine serum and L-glutamine and passaged every 3–5 days using 0.25% trypsin/EDTA (ThermoFisher Scientific). For fluorescence measurements of α3β2/α3β4, (henceforth known as α3-containing; α3*) and α7 nAChR activity, cells were plated at a density of 30,000 cells/well on 384-well black-walled imaging plates (Corning) 48 h, prior to FLIPR assays.

2.5. Fluorescence measurement of α7 and α3 nAChR activity*

Fluorescence measurement of α7 and α3* nAChR activity were performed using the FLIPR^{TETRA} fluorescence plate reader (Molecular Devices, Sunnyvale, CA) as previously described (Vetter and Lewis, 2010) In brief, SH-SY5Y cells were loaded with Calcium 4 no-wash dye (Molecular Devices) diluted in physiological salt solution with the following composition (in mM): NaCl 140, D-glucose 11.5, KCl 5.9, $MgCl_2$ 1.4, NaH_2PO_4 1.2, $NaHCO_3$ 5, $CaCl_2$ 1.8, HEPES 10, for 30 min at 37 °C. To assess activity of endogenously expressed human nAChR, fluorescence responses (excitation 470–495 nm; emission 515–575 nm) to addition of κ-HXTX-Hv1c were assessed for 5 min prior to stimulation

with agonist. Nicotine (30 µM) was used to activate endogenously expressed human α3* nAChRs, while endogenously expressed human α7 nAChRs were activated using the α7 nAChR agonist choline (30 µM) in the presence and absence of the positive allosteric modulator PNU120596 (10 µM). Raw fluorescence readings were converted to response over baseline using the analysis tool SCREENWORKS 3.1.1.4 (Molecular Devices) and were expressed relative to the maximum increase in fluorescence of control responses.

2.6. Data analyses

Patch-clamp data analyses were completed off-line following experimentation using AXOGRAPH X version 1.1 (Molecular Devices). Mathematical curve fitting was achieved using PRISM version 6.00c for Macintosh (GraphPad Software, San Diego, CA, USA). All curve-fitting routines were performed using non-linear regression analysis employing a least squares method. Comparisons of two sample means were made using a paired Student's *t*-test. Multiple comparisons were assessed by repeated measures of analysis of variance (ANOVA) with a Bonferroni's multiple comparison post-hoc test; differences were considered to be significant if $p < 0.05$. All data are presented as mean ± standard error of the mean (SEM) of *n* independent experiments, unless stated otherwise. The following equation was employed to fit current-voltage (*I-V*) curves:

$$I = g_{\max}\left(1-\left(\frac{1}{1+\exp\left[\left(V-V_{1/2}\right)/s\right]}\right)\right)\left(V-V_{\text{rev}}\right)$$

Where I is the amplitude of the peak current (either I_{Ba}, I_{Na}, I_{K}, $I_{\text{Glu-Cl}}$, $I_{\text{GABA-Cl}}$ or I_{nAChR}) at a given test potential V, $g_{\max}$ is the maximal conductance, $V_{1/2}$ is the voltage at half-maximal activation, s is the slope factor, and V_{rev} is the reversal potential.

Concentration-response curves were fitted using the following Logistic equation:

$$y = \frac{1}{1+\left([x]/IC_{50}\right)^{n_{\text{H}}}}$$

where x is the toxin dose, n_{H} is the Hill coefficient (slope parameter), and IC_{50} is the concentration at which 50% block of channel current is evident. In the case of concentration-response curves to a neurotransmitter, the IC_{50} value was substituted by ED_{50}; the agonist pulse duration that gives a half maximal response.

2.7. Source of chemicals

All chemicals were of analytical grade. Iberiotoxin, charybdotoxin, margatoxin, κ-SPRTX-Hv1b (formerly heteropodotoxin-2) and paxilline were purchased from Alomone Labs (Jerusalem, Israel).

$CaCl_2$ and $MgCl_2$ were obtained from Merck Chemicals (Kilsyth, Australia). BDS-I and κ-TRTX-Ps1a (formerly phrixotoxin-1) were generously provided by Dr Sylvie Diochot and Dr Pierre Escoubas, respectively (IPMC, CNRS, Valbonne, France). κ-HXTX-Hv1c was generously provided by Prof. Glenn King (Institute for Molecular Bioscience, University of Queensland, Australia). All remaining chemicals were purchased from Sigma-Aldrich (Castle Hill, Australia).

3. Results and Discussion

In the present study we obtained acute toxicity and electrophysiological data indicating that block of insect K_V4-like and/or $K_{Ca}1.1$ channels by κ-HXTX-Hv1c does not produce lethal effects in insects. We also report a novel action of κ-HXTX-Hv1c as a positive allosteric modulator (PAM) of insect nAChR, a known mode-of-action of current insecticides, which likely explains its neurotoxicity. Therefore κ-HXTX-Hv1c represents a promising lead compound in the development of insecticides targeting nAChR through a novel mechanism.

3.1. $K_{Ca}1.1$ channel toxins fail to induce insect lethality

Previous studies on cockroach DUM neurons indicate that the $K_{Ca}1.1$ channel is a target of **κ**-HXTX-Hv1c in insect neurons, however it remains to be proven whether block of this channel is in fact lethal to insects. We therefore assayed a number of $K_{Ca}1.1$ channel toxins for neurotoxic activity in house crickets, including the insect-selective κ-HXTX-Hv1c and classical $K_{Ca}1.1$ channel blockers including: paxilline, a non-peptidic tremorgenic indole alkaloid isolated from the fungus *Penicillium paxilli* (Cole et al., 1974); the well characterized but target non-selective ChTx (inhibits $K_{Ca}1.1$, $K_V1.2$, $K_V1.3$ and $K_V1.8$ channels; (Grissmer et al., 1994; Miller et al., 1985); and, the selective $K_{Ca}1.1$ channel blocker IbTx (Galvez et al., 1990). Both ChTx and IbTx have both been shown to potently inhibit $K_{Ca}1.1$ channels in cockroach DUM neurons (Windley et al., 2011; Gunning et al., 2008). Although the activities of paxilline have also been assessed on a number of mammalian $K_{Ca}1.1$ channels, little is understood concerning its acute toxicity in invertebrates.

Paxilline is one of the most potent non-peptide blockers of $K_{Ca}1.1$ channels in vertebrates (Sanchez and McManus, 1996) and was of importance to the present study as it has been shown to display insecticidal properties (Belofsky et al., 1995). Therefore, prior to assessing the neurotoxic effects of paxilline in insects it was essential to firstly confirm the inhibitory action of paxilline on $K_{Ca}1.1$ channels in cockroach DUM neurons. As expected, paxilline was found to potently block cockroach DUM neuron peak and late $I_{BK(Ca)}$ evoked at +30 mV with IC_{50} values of 13.6 ± 1.4 nM and 12.5 ± 1.7nM, respectively (n = 3–9; Fig. 1, A-B, F) with no overt effects on $I_{K(A)}$, $I_{K(DR)}$, $I_{K(Na)}$ (Figs. 1, C-G), I_{Ca} or I_{Na} (data not shown). Like IbTx, paxilline therefore appears to be a potent and selective blocker of both mammalian and insect $K_{Ca}1.1$ channels.

Figure 1 near here

Acute toxicity testing was carried out on house crickets following intrathoracic injections. High concentrations of paxilline up to 2 nmol/g failed to induce insect lethality. The volume of toxin added during acute toxicity experiments was equivalent to 5% of the cricket body weight. Assuming a 5% dilution, a 2 nmol/g toxin injection is equivalent to at least 100 nM in vivo, a concentration that should induce complete block of the target channel for each of the toxins tested.

Furthermore, acute toxicity testing of all three selective $K_{Ca}1.1$ channel blockers resulted in only minor signs of toxicity including twitching limbs and intermittent abdominal contractions, but at no time was there any paralysis or death due to these toxins. At toxin concentrations of 2–5 nmol/g no signs of toxicity were evident at time points beyond 2 h (Fig. 2A). These minor effects with classical $K_{Ca}1.1$ channel blockers are in contrast to the lethal neurotoxicity demonstrated by κ-HXTX-Hv1c at doses >10-fold lower in house crickets (LD_{50} 167 pmol/g after 48 h; (Wang et al., 2000). These results suggest that selective block of the insect $K_{Ca}1.1$ channel is not sufficient to induce the potent lethal effects demonstrated by κ-HXTX-Hv1c in insects.

Under current-clamp conditions, spontaneous action potentials were recorded from DUM neurons to assess whether κ-HXTX-Hv1c had any overt effects on action potential firing frequency. In the absence of any channel blockers, cells exhibited resting membrane potentials of –49.9 ± 1.0 mV (n = 52) and overshooting potentials of approximately +120 mV. In the presence of 100 nM κ-HXTX-Hv1c, spontaneous firing frequency showed a small but non-significant increase from 4.0 ± 0.6 Hz in controls (n = 52) to 6.0 ± 3.0 Hz in the presence of toxin (n = 4, p > 0.05; Fig. 2C, F). The resting membrane potential remained unaltered in the presence of 100 nM κ-HXTX-Hv1c (–54.1 ± 1.5 mV, n = 4, p > 0.05). Similar to κ-HXTX-Hv1c, 100 nM IbTx did not significantly alter spontaneous activity with a spike frequency of 4.4 ± 1.1 Hz (n = 7, p > 0.05, Fig. 2D, F). In agreement with previous reports (Grolleau and Lapied, 1995), it was evident that the $I_{K(A)}$ blocker, 4-AP, more significantly influenced action potential firing frequency. 4-AP is often used to isolate $I_{K(A)}$ in DUM neurons at low micromolar concentrations (Grolleau and Lapied, 1995) and was selected to assess the ability of $I_{K(A)}$ block to mimic the lethal, neurotoxic activity of κ-HXTX-Hv1c. Almost immediately following application of 5 mM 4-AP, firing frequency was increased to 12.1 ± 4.7 Hz (n = 5, p < 0.05; Fig. 2E-F). The ability of 4-AP to increase firing frequency is believed to be a consequence of enhanced sensitivity to stimulus evidenced by a reduction in the minimum refractory period (Grolleau and Lapied, 1995).

Figure 2 near here

3.2. Validation of K_A channels as a potential insecticidal target

Due to the reported modest effects of κ-HXTX-Hv1c on insect $I_{K(A)}$ (Gunning et al., 2008), and the notable increase in AP firing frequency in the presence of 4-AP, the potential of $I_{\mathbf{K(A)}}$ blockers to

induce neurotoxic symptoms in insects was also investigated. Acute insect toxicity testing in house crickets resulted in overt signs of neurotoxicity within 15 min following the injection of 4-AP at concentrations >100 nmol/g. Signs of neurotoxicity were initially characterized by twitching of legs and antennae and intermittent abdominal contractions. Within the first hour, symptoms progressed to uncoordinated movement and the absence of righting reflexes, characterized as knockdown, while at 48 h crickets were dead. At concentrations >100 nmol/g knockdown occurred within the first hour, while death was recorded at >24 h post injection. The 48 h KD_{50} and LD_{50} values for 4-AP were 410 ± 7 nmol/g and 496 ± 10 nmol/g, respectively (n = 3; Fig. 2A-B).

The progressive spastic paralysis, followed by a period of flaccid paralysis and death is reminiscent of the phenotype exhibited by κ-HXTX-Hv1c in a number of insects (Maggio and King, 2002a; Tedford et al., 2007; Wang et al., 2000). These results suggest that block of $I_{K(A)}$ may be sufficient to induce lethal neurotoxicity in insects, and therefore at least one of the channels responsible for the insect $I_{K(A)}$ may be the lethal target of κ-HXTX-Hv1c.

3.3. Effects of κ-HXTX-Hv1c on A-type transient K_V channel subtypes

The modest inhibition of $I_{K(A)}$ by κ-HXTX-Hv1c, highlights a K_A channel as a potential insecticidal target of κ-HXTX-Hv1c. Interestingly, no more than 30% inhibition of $I_{K(A)}$ was observed in the presence of κ-HXTX-Hv1c concentrations up to 5 μM (n = 5; Fig. 3A-B, D). This inhibition had a relative IC_{50} of 85 nM (n = 3), a value over 40-fold less potent than for inhibition of $K_{Ca}1.1$ channels in cockroach DUM neurons (Gunning et al., 2008). Similar to the inhibition of $K_{Ca}1.1$ channels, inhibition of $I_{K(A)}$ occurred without any significant changes in the voltage dependence of activation (Fig. 3C-D). To interpret these results, we considered the possibility that multiple K_V channel currents may contribute to $I_{K(A)}$ in cockroach DUM neurons, of which only one is sensitive to κ-HXTX-Hv1c.

Figure 3 near here

While it is known that several members of the Shaker channel family contribute to the K_V current in insects, the lack of selective blockers has made the identification of these channels difficult in native insect neurons (Grolleau and Lapied, 1995). Given the high sequence homology with the mammalian counterparts of these distinct families of K_V channels, we elected to test several known mammalian K_V channel blockers in insects. According to expression studies with *Drosophila* K_V channels, the *shal* and *shaker* genes appear to encode A-type transient K_V channel currents while the *shab* and *shaw* genes encode for delayed-rectifier channels with somewhat slower activation and inactivation kinetics (Covarrubias et al., 1991).

Initially, the selective K_V1 (Shaker-like) channel blocker margatoxin from the venom of the scorpion *Centruroides margaritatus* (Bednarek et al., 1994; Garcia-Calvo et al., 1993) was tested on DUM neuron $I_{K(A)}$. As illustrated in Fig. 4A, 1 μM margatoxin failed to alter the amplitude or kinetics of the $I_{K(A)}$ (4.0 ± 2.7% inhibition; n = 4, p > 0.05, pulse protocol 4G). Furthermore, margatoxin did

not alter the threshold of channel activation nor did it modify the $V_{1/2}$ (control = –31.2 ± 1.5 mV vs. margatoxin = –35.5 ± 3.2 mV; n = 3, p > 0.05, data not shown).

The K_V3 (Shaw-like) channel toxin BDS-I from the sea anemone (*Anemonia sulcata*) (Yeung et al., 2005) was tested on the DUM neuron K_A and K_{DR} currents using a dual pulse protocol to evoke channel currents. At concentrations up to 1 μM, BDS-I did not significantly alter the delayed-rectifier portion of the current recorded following a +30-mV voltage step (8.2 ± 2.3% decrease, n = 3, p > 0.05, Fig. 4B, G). Covarrubias and colleagues have shown that the *Drosophila* Shaw channel expressed in *Xenopus* oocytes possesses similar voltage-independent properties (Covarrubias et al., 1991) to the native $I_{K(DR)}$. This suggests that the major channel subtype responsible for mediating $I_{K(DR)}$ in cockroach DUM neurons is the K_V3-like Shaw channel. However, BDS-I either does not block insect Shaw channels or, with the limited amount of material at our disposal, the concentrations tested were insufficient.

As *shal* is believed to encode for the majority of transient K_V channels in embryonic *Drosophila* neurons (Tsunoda and Salkoff, 1995) the effects of K_V4 (Shal-like) channel blockers on $I_{K(A)}$ were examined. κ-TRTX-Ps1a (formerly phrixotoxin-1; (King et al., 2008) is known to block K_V4 and K_V2 (Shab-like) channels in vertebrates (Diochot et al., 1999). Given the high homology of κ-TRTX-Ps1a with the insecticidal $K_{Ca}1.1$ channel toxins isolated from the spider *Eucratoscelus constrictus* (Windley et al., 2011) and its ability to block mammalian K_V4 channels, this toxin was predicted to target DUM neuron $I_{K(A)}$. Using a dual prepulse protocol to evoke $I_{K(A)}$, the application of 200 nM κ-TRTX-Ps1a was found to reduce $I_{K(A)}$ by 20.6 ± 1.2% (n = 4; p < 0.05; Fig. 4C, G). In comparison, vertebrate $K_V4.3$ channels expressed in COS cells were almost completely abolished at concentrations greater than 200 nM (Diochot et al., 1999), suggesting that either insect K_V channels display differing sensitivity to their mammalian counterparts, or that the $I_{K(A)}$ of DUM neurons comprises of other K_V4-like (Shal) channels that remain relatively insensitive to the actions of κ-TRTX-Ps1a.

Although the effects of κ-TRTX-Ps1a on insect $I_{K(A)}$ were significant, they may represent a non-selective block of K_V2 (Shab) channels. Therefore, it was necessary to test a toxin known to selectively block mammalian K_V4 (Shal-like) channels that did not affect K_V2 (Shab-like) channels. κ-SPRTX-Hv1b (formerly heteropodotoxin-2) does not modulate the activity of Shaker, Shab or Shaw currents in vertebrates, nor does it inhibit mammalian Ca_V and Na_V channel currents (Sanguinetti et al., 1997). Application of 500 nM κ-SPRTX-Hv1b was found to block 23.9 ± 4.7% (n = 6, p < 0.05, Fig. 4D) of the $I_{K(A)}$ in DUM neurons. This appears to be a saturating concentration as a similar degree of block was also seen in the presence of 100 nM κ-SPRTX-Hv1b (24.4 ± 5.7%, n = 6, data not shown). Interestingly, the portion of $I_{K(A)}$ block correlated well with the results observed in the presence of κ-HXTX-Hv1c.

Fig. 4 near here

3.4. κ-HXTX-Hv1c and κ-SPRTX-Hv1b share a common insect target

To determine whether both κ-SPRTX-Hv1b and κ-HXTX-Hv1c block the same portion of $I_{K(A)}$, a number of co-application experiments were designed. Similar to previous experiments, $I_{K(A)}$ were evoked using a dual prepulse protocol and isolated following offline digital subtraction. Initially, DUM neurons were exposed to a saturating concentration of one toxin until equilibrium was achieved, after which a saturating concentration of the other toxin was added to the perfusion solution and the two toxins applied together (Gunning et al., 2008). $I_{K(A)}$ were recorded for a further 5 min to evaluate the occurrence of any additional current block. Following 23.9 ± 4.7% inhibition of $I_{K(A)}$ by 500 nM κ-SPRTX-Hv1b, subsequent application of 500 nM κ-HXTX-Hv1c failed to further inhibit the current, which remained at 23.0 ± 4.1% inhibition (n = 3, $p < 0.05$; Fig. 4E). In the complementary experiment, 500 nM κ-SPRTX-Hv1b also failed to cause further inhibition of $I_{K(A)}$ following exposure to 500 nM κ-HXTX-Hv1c (n = 3; Fig. 4F). These findings suggest that κ-HXTX-Hv1c inhibits the same channel as the established selective K_V4 blocker κ-SPRTX-Hv1b. Therefore, we propose that κ-HXTX-Hv1c blocks the K_V4 channel equivalent to Shal in insects (Butler et al., 1989; Wei et al., 1990).

3.5. K_A and $K_{Ca}1.1$ channel toxins are not lethal in crickets

Subsequently, acute insect toxicity assays were used to assess the neurotoxicity of K_V4 (Shal-like) channel blockers in house crickets. No neurotoxic symptoms were observed following the injection of up to 5 nmol/g of κ-SPRTX-Hv1b at a 48-h endpoint (Fig. 2A). To eliminate the possibility of an obligate relationship where both $K_{Ca}1.1$ and K_V4-like channel block are required for insecticidal activity, insects were also simultaneously injected with κ-SPRTX-Hv1b and the selective $K_{Ca}1.1$ channel blocker IbTx, in a 1:1 stoichiometry. Again, following injection of doses up to 2 nmol/g of each toxin, the crickets failed to exhibit any overt signs of neurotoxicity (Fig. 2A). The lethal effects of 4-AP in insects are most likely explained by combined block of $I_{K(A)}$ (including K_V1 and Kv4) and other voltage-gated channels, such as K_{Na} (Covarrubias et al., 1991; Gasque et al., 2005; Peng and Wu, 2007; Stocker et al., 1990; Wei et al., 1990). Subsequently, the results of this study indicate that block of K_V4-like channels alone or in combination with $K_{Ca}1.1$ is not sufficient to result in the insecticidal activity induced by κ-HXTX-Hv1c.

3.6. Minor effects of κ-HXTX-Hv1c on K_{Na} channel currents

Of the K_V channels known to be present in cockroach DUM neurons (Grolleau and Lapied, 1994; Grolleau and Lapied, 1995), only the K_{Na} channel remained untested as a potential target of κ-HXTX-Hv1c. Accordingly, K_{Na} channel currents in DUM neurons were elicited in the presence of the inward I_{Na} and isolated through offline subtraction routines (Fig. 5A, C; see methods for further details).

Unfortunately 4-AP could not be used to block $I_{K(A)}$ as it also inhibits $I_{K(Na)}$ (Grolleau and Lapied, 1994; Wicher et al., 2001). The absence of $I_{K(A)}$ block when recording K_{Na} channel currents causes somewhat of a dilemma given the reported modest inhibition of $I_{K(A)}$ by κ-HXTX-Hv1c in DUM neurons. In the presence of 1 μM κ-HXTX-Hv1c K_{Na} currents were reduced by 27.6 ± 9.3% (n = 4, p < 0.05; Fig. 5B). Due to the presence of $I_{K(A)}$, moderate block of K_{Na} in the presence of κ-HXTX-Hv1c does not necessarily confirm or eliminate this channel as a possible target. However, the current inhibition does not appear to be substantially greater than the 24.9 ± 3.6% (n = 4, p < 0.05) $I_{K(A)}$ inhibition at –10 mV (Fig. 3C). These results further highlight the need to identify more selective toxins for the isolation of channel currents in native insect neurons.

Figure 5 near here

3.7. Effects of κ-HXTX-Hv1c on nACh receptor currents

Several other potential targets are capable of mediating rapid neurotoxicity in insects, including the neurotransmitter-gated nACh, Glu-Cl and GABA receptors. In a further attempt to identify the lethal target of κ-HXTX-Hv1c we tested the effects of the toxin on DUM neuron nAChRs. In cockroach DUM neurons from the terminal abdominal ganglion application of nicotinic agonists results in a biphasic response characterised by fast and slow components (Lapied et al., 1990). We found that concentrations up to 1 μM κ-HXTX-Hv1c failed to significantly affect the amplitude or decay rate of the fast (0–700 ms) transient desensitizing I_{nAChR} (n = 5, p > 0.05; Fig. 6A-B and 7A), however, within 5 min of toxin application, κ-HXTX-Hv1c produce a concentration-dependent slowing of the decay rates of the slow (>700 ms) non-desensitizing I_{nAChR} (Fig. 7B).

In addition, an apparent slower secondary I_{nAChR} component following partial decay of the current became prominent post-toxin application and visible as a second peak during the slow non-desensitizing I_{nAChR}. This second peak was more apparent at higher toxin concentrations (> 200 nM) as the effects of κ-HXTX-Hv1c to slow the rate of non-desensitizing current decay were enhanced (Fig. 6C, blue circle). In the presence of 500 nM κ-HXTX-Hv1c, a 9.9 ± 1.0-fold (n = 5, p < 0.05) increase in the amplitude of this secondary component was evident. Measurements were taken at the maximum amplitude (Fig. 6C) in response to toxin and compared with control amplitudes at the same time point. Importantly, κ-HXTX-Hv1c failed to induce a current when applied directly to DUM neurons at concentrations up to 1 μM (Fig. 6D), indicating that the toxin was not capable of directly activating I_{nAChR}.

Figure 6 near here

3.7.1. κ-HXTX-Hv1c prolongs nAChR current decay

To compare data at varying concentrations of κ-HXTX-Hv1c, the current duration was measured at 20% of peak transient I_{nAChR} amplitude (t_{20}, Fig. 6C). We chose to measure the t_{20} value in the present study, rather than fitting exponential functions to the current decay, as no fewer than four components were required, consistent with the suggestion of at least four ACh receptor subtypes in cockroach DUM neurons (see below). Control currents evoked in response to 10-ms pulses of 10 μM nicotine decayed with a t_{20} of 2.2 ± 0.3 s (n = 27) reflecting mainly the late non-desensitizing I_{nAChR}, while t_{20} values in the presence of 500 nM and 1 μM κ-HXTX-Hv1c were increased to 9.8 ± 3.6 s (n = 6, p < 0.001) and 8.2 ± 1.8 s (n = 4, p < 0.001), respectively (data shown as a fold-increase over control t_{20}, Fig. 7B). The duration of current decay was increased by κ-HXTX-Hv1c in an concentration-dependent manner with an ED_{50} of 180.1 ± 30.4 nM and a maximum increase of 4.7 ± 3.2-fold in the presence of 500 nM toxin (n = 4–6; Fig. 7B).

To identify any modulation of nAChR agonist sensitivity we examined the ability of 200 nM κ-HXTX-Hv1c to prolong current decay in response to varying durations of nicotine application. Duration measurements taken at t_{20} at a given nicotine pulse duration were compared in the absence and presence of κ-HXTX-Hv1c. Despite the dramatic increase in the t_{20} value, no significant shift in the nicotine duration-response curve was observed following κ-HXTX-Hv1c application (ED_{50} = 6.6 ± 0.5 ms in comparison to 8.5 ± 0.5 ms for control, n = 3, p > 0.05; Fig. 7C). In addition, there were no voltage-dependent effects on the amplitude of nAChR currents evoked by 10 μM nicotine (n = 3; Fig. 7D).

Figure 7 near here

The results of this study indicate that the fast transient, rapidly desensitizing portion of the nAChR current is largely unaffected by κ-HXTX-Hv1c while the slow non-desensitizing component of the nAChR undergoes significant slowing of current decay. Moreover, a clear increase in the initial portion of the slow non-desensitizing current, particularly in the presence of high concentrations of κ-HXTX-Hv1c, might mask an enhancement of a component, which is obscured by the initial transient current.

Investigations on cockroach DUM neurons from the terminal abdominal ganglion have identified the presence of multiple nAChR channel subtypes. These vary between the α-BgTx-resistant fast desensitizing (nAChD) and α-BgTx-sensitive slow non-desensitizing current (nAChN) components of the I_{nAChR} (Courjaret and Lapied, 2001; Lapied et al., 1990). The α-BgTx-resistant nAChR subtypes are characterised as nAChR1 and nAChR2 receptors based on differing ion permeation and pharmacological properties (Courjaret and Lapied, 2001). Studies have found that nAChR1 is selectively blocked by *d*-tubocurarine, while nAChR2 is preferentially blocked by mecamylamine and the mammalian α7 nAChR blocker, α-conotoxin ImI (Courjaret and Lapied, 2001). However, in the present study κ-HXTX-Hv1c targeted the slow non-desensitizing nAChR current component. The

identification of this component was confirmed in the present study by the addition of 500 µM α-BgTx, which resulted in a modest block (Fig. 7A) of the slow non-desensitizing component of the DUM neuron I_{nAChR} (Fig. 6D). In cockroach DUM neurons, this α-BgTx-sensitive nAChN component includes channel subtypes with 'mixed' nicotinic and muscarinic activity, where the antagonists α-BgTx (nicotinic) as well as pirenzepine (M1) and gallamine (M2) all inhibiting the non-desensitizing I_{nAChR}, whereas the fast nAChD component is insensitive to these antagonists (Lapied et al., 1990).

In comparison to vertebrate nAChRs, insect gene families are relatively small with diversity created through alternative splicing (Jones et al., 2005; Lansdell and Millar, 2000). Insect nAChRs consist of of homopentameric α-subunits or heteropentameric α- and β-subunits that are highly conserved with greater than 60% identity between species and as high as 80% for the α1 subunit (Jones et al., 2007). A total of 10 genes have been identified in insects, nominally α1-α7 and β1-β3 in order of discovery, however in reality fewer likely form functional receptors (Jonas et al., 1990.; Lansdell and Millar, 2000; Littleton and Ganetzky, 2000; Schulz et al., 1998). Unfortunately, while the successful cloning of various nAChR subunits has been reported in several insect species, few have been functionally expressed (Eastham et al., 1998; Gao et al., 2007; Hermsen et al., 1998; Millar and Lansdell, 2010). Importantly, these insect subunits possess relatively low homology with vertebrates, most exhibiting only 30-40% homology with mammalian α2 or α7 subunits (Jones and Sattelle, 2010). The lack of homology with vertebrate receptors likely explains the relative insect selectivity of insecticides that target nAChRs (for a review see Tomizawa and Casida, 2003).

3.7.2. κ-HXTX-Hv1c reverses insect nAChR channel desensitization

Given that κ-HXTX-Hv1c slowed the rate of I_{nAChR} decay, we explored if the mechanism was related to changes in nACh receptor desensitization. nAChR desensitization is exhibited as a reduction in response to continuous application of nicotine and this process is reversible following agonist removal (Katz and Thesleff, 1957; Quick and Lester, 2002). Following a 100 s continuous application of nicotine, I_{nAChR} amplitude was found to reach 19.5 ± 5% of maximum amplitude as a result of receptor desensitization (n = 6; Fig. 8A). Although slight differences were seen in the initial I_{nAChR} decay timecourse (Fig. 8A-D), this variability is most likely due to the mixed population of nAChR subtypes present in DUM neurons (Bai and Sattelle, 1993; Courjaret and Lapied, 2001; Lapied et al., 1990; Salgado and Saar, 2004). Regardless of the decay time-course of control I_{nAChR} in response to continuous application of nicotine, subsequent co-application of toxin and nicotine caused an increase in the late I_{nAChR} amplitude thus partially reversing nACh receptor desensitization. Application of EC_{50} concentrations of κ-HXTX-Hv1c (200 nM) following partial (~80%) I_{nAChR} desensitization recovered 32.6 ± 2.9% of I_{nAChR} amplitude (n = 2; Fig. 8B) and 500 nM κ-HXTX-Hv1c caused a 33.7 ± 15.7% recovery of I_{nAChR} amplitude (n = 3; Fig. 8C and D), while application of control solution failed to alter current amplitude (Fig. 8A). Importantly, cessation of nicotine perfusion and continued application of

toxin resulted in the reduction of I_{nAChR} likely representing channel closure (Fig. 8B-D). Furthermore, κ-HXTX-Hv1c did not directly activate I_{nAChR} at concentrations up to 1 μM (data not shown). This indicates that the presence of both agonist and toxin are required to reverse desensitization.

These findings are consistent with actions of positive allosteric modulators (PAMs) on the nAChR (Arias et al., 2011; Barron et al., 2009; Bertrand et al., 2008; Gronlien et al., 2007). Furthermore, based on the ability of κ-HXTX-Hv1c to both prolong current decay and alter nAChR desensitization this toxin is likely to act as a type II PAM (Bertrand and Gopalakrishnan, 2007).

Figure 8 near here

In this study we probed two features of nAChR modulation by κ-HXTX-Hv1c, current decay in response to short pulses of nicotine and reactivation of desensitized receptors to gauge effects on resting (closed channel, no agonist); active (open channel briefly stabilized by agonist); and, desensitized (closed, stabilized in the prolonged presence of agonist) states (Bertrand and Gopalakrishnan, 2007). Short pulses of nicotine (10 ms) briefly stabilize the open state of the channel and results in relatively low levels of desensitization, allowing the rate of channel recovery to be determined following agonist removal. The rate of decay of this early phase of the I_{nAChR} was not significantly altered in the present of κ-HXTX-Hv1c, however, κ-HXTX-Hv1c did cause a prolongation of the late phase of I_{nAChR} decay (Fig. 6C). Thus, κ-HXTX-Hv1c may act like the type II PAM PNU-1205996 (Wang et al., 2015) by stabilizing the open state and prolonging channel opening. This secondary slower component has also been observed with other nAChR type II PAMs, where it has been attributed to the ability of the transmitter to reach the orthosteric site faster than the PAM reaches the allosteric site (Gill et al., 2012). However, this explanation seems unlikely since the currents were recorded in the sustained presence of toxin with intermittent exposure to nicotine. More likely is the toxin has a differential action on slow non-desensitizing nAChRs, in comparison to fast desensitizing nAChR channel subtypes contributing to the insect I_{nAChR} (Salgado and Saar, 2004).

In the continued presence of nicotine, a population of mostly fully desensitized channels seems to be reactivated in the presence of κ-HXTX-Hv1c (Fig. 8B-D). This suggests that κ-HXTX-Hv1c reactivates channels by destabilizing the desensitized state, increasing the rate of transition to the open state. This potential mechanism has been previously postulated for type II PAMs (Wang et al., 2015). However, an in-depth characterization of κ-HXTX-Hv1c on the yet uncharacterized insect nAChR subtypes comprising the slow non-desensitizing current that contribute to cockroach DUM neuron I_{nAChR} is required to fully elucidate the molecular mechanisms underlying the effects of κ-HXTX-Hv1c on these receptors. Importantly, slow non-desensitizing nAChN receptors are the target for a number of insecticides including neonicotinoids and spinosad (Salgado and Saar, 2004). Indeed, insecticides targeting nAChRs make up approximately a third of the global insecticide market with neonicotinoids and spinosad contributing a major portion (Simon-Delso et al., 2015). Importantly spinosyn A, the active component of spinosad, acts allosterically as a PAM of slow non-desensitizing nAChN

receptors (Salgado and Saar, 2004), in a similar manner to κ-HXTX-Hv1c, lending further support to the argument that the lethal target of κ-HXTX-Hv1c is the nAChR.

3.8. GABA and glutamate gated chloride channels are not targeted by κ-HXTX-Hv1c

In order to confirm that κ-HXTX-Hv1c selectively targeted the nAChR and not other major neurotransmitter receptors in insects we tested the effects on GABA and glutamate chloride channels. To assess the effects of κ-HXTX-Hv1c on Glu-Cl channels, inward $I_{Glu\text{-}Cl}$ were evoked by 40-ms pulses of 100 μM glutamate. In the presence of 1 μM κ-HXTX-Hv1c, $I_{Glu\text{-}Cl}$ peak amplitude was increased 1.2 ± 0.08-fold (n = 4, p < 0.05; Fig. 9A, C) while at 50 nM currents were only increased 1.08 ± 0.03-fold (n = 3, p > 0.05; Fig. 9C). Increases in amplitude were evident within 2 min of toxin application. $I_{Glu\text{-}Cl}$ duration at 20% of maximal peak amplitude (t_{20}) was not significantly altered at concentrations of κ-HXTX-Hv1c up to 1 μM (n = 3–4, p > 0.05; 9D). As a positive control we applied 100 nM picrotoxin, which blocks DUM neuron Glu-Cl channel currents (n = 3; p <0.05, Fig. 9B, C).

Due to the effects of κ-HXTX-Hv1c on $I_{Glu\text{-}Cl}$ amplitude, the sensitivity of Glu-Cl channels to glutamate was assessed. Peak $I_{Glu\text{-}Cl}$ amplitude was recorded in response to varying pulse durations of 100 μM glutamate in the absence and presence of toxin (Fig. 9E). Prior to toxin perfusion the data yielded an ED_{50} of 17.8 ± 1.4 ms while the ED_{50} value was reduced to 12.6 ± 3.4 ms in the presence of 1 μM κ-HXTX-Hv1c (n = 5, p < 0.05; Fig. 9F). Peak $I_{Glu\text{-}Cl}$ amplitude was increased at all pulse durations of glutamate tested in the presence of toxin (Figure 9E-F) and thus the amplitude of $I_{Glu\text{-}Cl}$ was increased beyond the maximum amplitude achieved under control conditions (i.e. at pulse durations >320 ms).

Despite these significant but modest actions on $I_{Glu\text{-}Cl}$, it is unlikely that an enhancement of an inhibitory response (Cleland, 1996; de Figueiredo et al., 2001) is responsible for the potent *excitatory* neurotoxicity caused by κ-HXTX-Hv1c. Furthermore, a significant enhancement of $I_{Glu\text{-}Cl}$ amplitude (p < 0.05) was only evident at a concentration of 1 μM, which seems unlikely to be effective enough to correlate with the potent toxicity seen in insect bioassays (Gunning et al., 2008; Maggio and King, 2002b; Tedford et al., 2007; Wang et al., 2000).

Figure 9 near here

The effects of κ-HXTX-Hv1c were also assessed on $I_{GABA\text{-}Cl}$. In the presence of 1 μM toxin, $I_{GABA\text{-}Cl}$ evoked by 100-ms pulses of GABA remained unaltered (Fig. 10A). $I_{GABA\text{-}Cl}$ were recorded in the presence of toxin (100 nM and 1 μM) for up to 10 min however no significant changes in $I_{GABA\text{-}Cl}$ amplitude or duration were observed (n = 4–5, p > 0.05; Fig. 10C, D). In comparison, 100 μM picrotoxin, a known inhibitor of $I_{GABA\text{-}Cl}$, resulted in significant a significant level of block (n = 3; p < 0.05; Fig. 10B, C). Therefore, the effects of κ-HXTX-Hv1c on chloride currents appear to be limited to those mediated by glutamate.

3.9. κ-HXTX-Hv1c does not modulate vertebrate α7 and α3* nAChRs

To confirm that the effect of κ-HXTX-Hv1c on nAChRs was selective for insects, calcium responses of vertebrate α7 and α3β2/α3β4 nAChR were assessed in a FLIPR assay. These receptor stoichiometries were selected as the CNS α7 and α3β2, as well as the peripherally located α3β4, receptors represent the most common neuronal nAChR subtypes found in the vertebrate nervous system, and the vertebrate α7 has been previously used in assays to determine the efficacy and selectivity of neonicotinoid insecticides (Ihara et al., 2003). When challenged with nicotine, the calcium responses of endogenously expressed vertebrate α3* nAChR also remained unchanged in the presence of increasing concentrations of κ-HXTX-Hv1c (n = 3, p > 0.05; Fig. 11B), while in the presence of *d*-tubocurarine α3* nAChR calcium responses were inhibited with an IC_{50} of 8.7 ± 1.1 μM (n = 3; Fig. 11B). κ-HXTX-Hv1c also failed to activate either α3* or α7 human nAChRs directly despite the ability of the type II PAM, PNU120596, to enhance the α3* response to nicotine (Fig. 11C) or the α7 response to choline (Mueller et al., 2015). Vertebrate α7 nAChR calcium responses evoked by choline in the presence of PNU120596 were additionally unaffected in the presence of κ-HXTX-Hv1c (n = 3, p > 0.05, Fig. 11A). It should be noted that due to the small size of α7 receptor responses in this expression system, they were recorded in the presence of the type II PAM, PNU120596. This may be problematic since PNU120596 exhibits similar actions on mammalian α7 nAChR (Wang et al., 2015) as κ-HXTX-Hv1c does on insect nAChRs. However, κ-HXTX-Hv1c failed to enhance the response to choline, like PNU120596, and given that these receptors are exclusively found in the CNS it is unlikely that a large peptide toxin like κ-HXTX-Hv1c would be able to cross the vertebrate blood brain barrier to reach the target receptor. Moreover, we have confirmed that κ-HXTX-Hv1c does not target peripheral human nAChR stoichiometries (α3*), further supporting the phyla selectivity of this toxin for insects.

Figure 11 near here

3.10. Validation of nAChR as a lethal target

The insect nAChR is already recognised as an insecticidal target (Millar and Denholm, 2007) with a number of commercially available insecticides that enhance (imidacloprid; Bai et al., 1991), inhibit (cartap; Lee et al., 2003) or allosterically modulate (spinosad; Salgado and Saar, 2004) insect nAChR receptor function. In support of the positive allosteric modulation of nAChR and its ability to induce lethal actions in insects, κ-HXTX-Hv1c appears to have a mode of action similar to the excitatory insecticide spinosyn A (Salgado, 1998; Salgado and Saar, 2004; Salgado et al., 1998; Watson et al., 2010). Moreover, studies have indicated that spinosyn A (the major component of spinosad) interacts with a site on insect nAChRs that is distinct from other insecticides (Salgado and

Saar, 2004) and subsequently is not under high selection pressure that might contribute to the rapid development of insect resistance. While spinosad additionally enhances GABA receptor activity in some insect species, the effect on nAChRs alone is considered to be sufficient to induce excitatory insecticidal activity (Orr et al., 2009; Salgado and Sparks, 2005). Given κ-HXTX-Hv1c has weak to no activity on GABA receptors, we believe that positive allosteric modulation of the nAChR alone explains the excitatory neurotoxic phenotype observed in insects following exposure to κ-HXTX-Hv1c.

Due to the modest effects of κ-HXTX-Hv1c on action potential firing frequency in the cockroach neurons, we believe that while block of $K_{Ca}1.1$ and K_V4-like channels are not lethal, they may play a supporting role in the development of neurotoxicity in insects. The increase in firing frequency induced by $K_{Ca}1.1$ and K_V4-like channel block may well play a synergistic role with the positive allosteric modulation of nAChR by increasing neurotransmitter release to further enhance excitotoxicity in the insect nervous system. However, as inhibition of $K_{Ca}1.1$ and/or K_V4-like channels are not lethal it is unlikely that the effects on these channels are directly related to the allosteric modulation of nAChRs.

κ-HXTX-Hv1c is the first spider peptide toxin characterized to target the insect nAChR (See ArachnoServer database; Herzig et al., 2011). Although insect nAChRs are not new targets for insecticides (Millar and Denholm, 2007) κ-HXTX-Hv1c exhibits a novel mode of action as a positive allosteric modulator and therefore is likely to interact with a unique site on this receptor (Bertrand et al., 2008). Moreover, given its novel mode of action, κ-HXTX-Hv1c may help alleviate insect resistance to other nAChR agrochemicals that partially activate nAChRs such as imidacloprid (Buckingham et al., 1997). In support, studies have shown that pyrethroid-resistant strains were more sensitive to insecticides that bound to the channel at different locations than pyrethroids (McCutchen et al., 1997). This suggests that if κ-HXTX-Hv1c targets a different site on the same nAChR as commercially available insecticides it may be a useful tool in the control of insecticide resistance.

4. Conclusions

In conclusion, κ-HXTX-Hv1c is an insect-selective positive allosteric modulator of insect slow non-desensitizing nACh receptors. This activity is consistent with the lethal excitatory activity of κ-HXTX-Hv1c in insects, and is potentially enhanced by the additional block of insect $K_{Ca}1.1$ and K_V4-like channels. κ-HXTX-Hv1c is therefore an ideal lead compound for the development of novel insecticides and may also be a useful tool in an integrated pest management approach to preventing insect resistance against existing agrochemicals targeting nicotinic receptors. An improved understanding of the complexity of nAChR subtypes present in insects, particularly those involved in the slow non-desensitizing nACh receptor current will be necessary to further understand the

mechanism and site of action of κ-HXTX-Hv1c on the nAChR and to aid in the design of new insecticides.

5. References

Arias HR, Gu R-X, Feuerbach D, Guo B-B, Ye Y and Wei D-Q (2011) Novel positive allosteric modulators of the human α7 nicotinic acetylcholine receptor. *Biochemistry* **50**(23): 5263-5278.

Bai D, Lummis SCR, Leicht W, Breer H and Sattelle DB (1991) Actions of imidacloprid and a related nitromethylene on cholinergic receptors of an identified insect motor neurone. *Pesticide Science* **33**: 197-204.

Bai D and Sattelle DB (1993) Neosurugatoxin blocks an alpha-bungarotoxin-sensitive neuronal nicotinic acetylcholine receptor. *Archives of insect biochemistry and physiology* **23**(4): 161-167.

Barron SC, McLaughlin JT, See JA, Richards VL and Rosenberg RL (2009) An allosteric modulator of α7 nicotinic receptors, N-(5-chloro-2,4-dimethoxyphenyl)-N'-(5-methyl-3-isoxazolyl)-urea (PNU-120596), causes conformational changes in the extracellular ligand binding domain similar to those caused by acetylcholine. *Molecular pharmacology* **76**(2): 253-263.

Barry PH (1994) JPCalc, a software package for calculating liquid junction potential corrections in patch-clamp, intracellular, epithelial and bilayer measurements and for correcting junction potential measurements. *Journal of Neuroscience Methods* **51**(1): 107-116.

Bednarek MA, Bugianesi RM, Leonard RJ and Felix JP (1994) Chemical synthesis and structure-function studies of margatoxin, a potent inhibitor of voltage-dependent potassium channel in human T lymphocytes. *Biochemical and biophysical research communications* **198**(2): 619-625.

Belofsky GN, Gloer JB, Wicklow DT and Dowd PF (1995) Antiinsectan alkaloids: Shearinines A-C and a new paxilline derivative from the ascostromata of *Eupenicillium shearii*. *Tetrahedron* **51**(14): 3959-3968.

Bertrand D, Bertrand S, Cassar S, Gubbins E, Li J and Gopalakrishnan M (2008) Positive allosteric modulation of the α7 nicotinic acetylcholine receptor: ligand interactions with distinct binding sites and evidence for a prominent role of the M2-M3 segment. *Molecular pharmacology* **74**(5): 1407-1416.

Bertrand D and Gopalakrishnan M (2007) Allosteric modulation of nicotinic acetylcholine receptors. *Biochemical Pharmacology* **74**(8): 1155-1163.

Bodereau-Dubois B, List O, Calas-List D, Marques O, Communal PY, Thany SH and Lapied B (2012) Transmembrane potential polarization, calcium influx, and receptor conformational state modulate the sensitivity of the imidacloprid-insensitive neuronal insect nicotinic acetylcholine receptor to neonicotinoid insecticides. *J Pharmacol Exp Ther* **341**(2): 326-339.

Buckingham S, Lapied B, Corronc H and Sattelle F (1997) Imidacloprid actions on insect neuronal acetylcholine receptors. *Journal of Experimental Biology* **200**(21): 2685-2692.

Butler A, Wei AG, Baker K and Salkoff L (1989) A family of putative potassium channel genes in Drosophila. *Science* **243**(4893): 943-947.

Cleland T (1996) Inhibitory glutamate receptor channels. *Molecular Neurobiology* **13**(2): 97-136.

Cole RJ, Kirksey JW and Wells JM (1974) A new tremorgenic metabolite from *Penicillium paxilli*. *Canadian Journal of Microbiology* **20**(8): 1159-1162.

Courjaret R, Grolleau F and Lapied B (2003) Two distinct calcium-sensitive and -insensitive PKC up- and down-regulate an α-bungarotoxin-resistant nAChR1 in insect neurosecretory cells (DUM neurons). *European Journal of Neuroscience* **17**(10): 2023-2034.

Courjaret R and Lapied B (2001) Complex intracellular messenger pathways regulate one type of neuronal alpha-bungarotoxin-resistant nicotinic acetylcholine receptors expressed in insect neurosecretory cells (dorsal unpaired median neurons). *Molecular pharmacology* **60**(1): 80-91.

Covarrubias M, Wei A and Salkoff L (1991) Shaker, Shal, Shab, and Shaw express independent K^+ current systems. *Neuron* **7**(5): 763-773.

de Figueiredo SG, de Lima ME, Nascimento Cordeiro M, Diniz CR, Patten D, Halliwell RF, Gilroy J and Richardson M (2001) Purification and amino acid sequence of a highly insecticidal toxin from the venom of the brazilian spider *Phoneutria nigriventer* which inhibits NMDA-evoked currents in rat hippocampal neurones. *Toxicon* **39**(2-3): 309-317.

Diochot S, Drici M-D, Moinier D, Fink M and Lazdunski M (1999) Effects of phrixotoxins on the K_V4 family of potassium channels and implications for the role of I_{to1} in cardiac electrogenesis. *British Journal of Pharmacology* **126**: 251-263.

Eastham HM, Lind RJ, Eastlake JL, Clarke BS, Towner P, Reynolds SE, Wolstenholme AJ and Wonnacott S (1998) Characterization of a nicotinic acetylcholine receptor from the insect Manduca sexta. *Eur J Neurosci* **10**(3): 879-889.

Elkins T, Ganetzky B and Wu CF (1986) A Drosophila mutation that eliminates a calcium-dependent potassium current. *Proc Natl Acad Sci U S A* **83**(21): 8415-8419.

Galvez A, Gimenez-Gallego G, Reuben JP, Roy-Contancin L, Feigenbaum P, Kaczorowski GJ and Garcia ML (1990) Purification and characterization of a unique, potent, peptidyl probe for the high conductance calcium-activated potassium channel from venom of the scorpion Buthus tamulus. *The Journal of biological chemistry* **265**(19): 11083-11090.

Gao JR, Deacutis JM and Scott JG (2007) Characterization of the nicotinic acetylcholine receptor subunit gene Mdalpha2 from the house fly, Musca domestica. *Arch Insect Biochem Physiol* **64**(1): 30-42.

Garcia-Calvo M, Leonard RJ, Novick J, Stevens SP, Schmalhofer W, Kaczorowski GJ and Garcia ML (1993) Purification, characterization, and biosynthesis of margatoxin, a component of Centruroides margaritatus venom that selectively inhibits voltage-dependent potassium channels. *Journal of Biological Chemistry* **268**(25): 18866-18874.

Gasque G, Labarca P, Reynaud E and Darszon A (2005) Shal and Shaker differential contribution to the K^+ currents in the *Drosophila* mushroom body neurons. *Journal of Neuroscience* **25**(9): 2348 -2358.

Gill JK, Dhankher P, Sheppard TD, Sher E and Millar NS (2012) A series of alpha7 nicotinic acetylcholine receptor allosteric modulators with close chemical similarity but diverse pharmacological properties. *Mol Pharmacol* **81**(5): 710-718.

Grissmer S, Nguyen AN, Aiyar J, Hanson DC, Mather RJ, Gutman GA, Karmilowicz MJ, Auperin DD and Chandy KG (1994) Pharmacological characterization of five cloned voltage-gated K+ channels, types Kv1.1, 1.2, 1.3, 1.5, and 3.1, stably expressed in mammalian cell lines. *Molecular pharmacology* **45**(6): 1227-1234.

Grolleau F and Lapied B (1994) Transient Na^+-activated K^+ current in beating pacemaker-isolated adult insect neurosecretory cells (DUM neurones). *Neuroscience Letters* **167**(1-2): 46-50.

Grolleau F and Lapied B (1995) Separation and identification of multiple potassium currents regulating the pacemaker activity of insect neurosecretory cells (DUM neurons). *Journal of Neurophysiology* **73**: 160-171.

Grolleau F and Lapied B (2000) Dorsal unpaired median neurons in the insect central nervous system: towards a better understanding of the ionic mechanisms underlying spontaneous electrical activity. *Journal of Experimental Biology* **203**: 1633-1648.

Gronlien J, Hakerud M, Ween H, Thorin-Hagene K, Briggs CA, Gopalakrishnan M and Malysz J (2007) Distinct profiles of α7 nAChR positive allosteric modulation revealed by structurally diverse chemotypes. *Molecular pharmacology* **72**(3): 715-724.

Gunning SJ, Maggio F, Windley MJ, Valenzuela SM, King GF and Nicholson GM (2008) The Janus-faced atracotoxins are specific blockers of invertebrate K_{Ca} channels. *FEBS Letters* **275**(16): 4045-4059.

Hamill OP, Marty A, Neher E, Sakmann B and Sigworth FJ (1981) Improved patch-clamp techniques for high-resolution current recording from cells and cell-free membrane patches. *Pflügers Archiv (Eur J Physiol)* **391**: 85–100.

Hermsen B, Stetzer E, Thees R, Heiermann R, Schrattenholz A, Ebbinghaus U, Kretschmer A, Methfessel C, Reinhardt S and Maelicke A (1998) Neuronal nicotinic receptors in the locust Locusta migratoria. Cloning and expression. *J Biol Chem* **273**(29): 18394-18404.

Herzig V, Wood DLA, Newell F, Chaumeil P-A, Kaas Q, Binford GJ, Nicholson GM, Gorse D and King GF (2011) Arachnoserver 2.0, an updated online resource for spider toxin sequences and structures. *Nucleic Acids Research* **39**(Suppl 1): D653-D657.

Jonas P, Baumann A, Merz B and Gundelfinger ED (1990.) Structure and developmental expression of the Dα2 gene encoding a novel nicotinic acetylcholine receptor protein of Drosophila melanogaster. . *FEBS Letters* **269**: 264–268.

Jones AK, Brown LA and Sattelle DB (2007) Insect nicotinic acetylcholine receptor gene families: from genetic model organism to vector, pest and beneficial species. *Invert Neurosci* **7**(1): 67-73.

Jones AK, Grauso M and Sattelle DB (2005) The nicotinic acetylcholine receptor gene family of the malaria mosquito, Anopheles gambiae. *Genomics* **85**(2): 176-187.

Jones AK and Sattelle DB (2010) Diversity of insect nicotinic acetylcholine receptor subunits. *Adv Exp Med Biol* **683**: 25-43.

Katz B and Thesleff S (1957) A study of the desensitization produced by acetylcholine at the motor end-plate. *J Physiol* **138**(1): 63-80.

King GF, Gentza MC, Escoubas P and Nicholson GM (2008) A rational nomenclature for naming peptide toxins from spiders and other venomous animals. *Toxicon* **52**(2): 264–276.

Lansdell SJ and Millar NS (2000) Cloning and heterologous expression of Dalpha4, a Drosophila neuronal nicotinic acetylcholine receptor subunit: identification of an alternative exon influencing the efficiency of subunit assembly. *Neuropharmacology* **39**(13): 2604-2614.

Lapied B, Corronc H and Hue B (1990) Sensitive nicotinic and mixed nicotinic-muscarinic receptors in insect neurosecretory cells. *Brain Research* **533**: 132-136.

Lapied B, Malecot CO and Pelhate M (1989) Ionic species involved in the electrical activity of single aminergic neurones isolated from the sixth abdominal ganglion of the cockroach *Periplaneta americana*. *Journal of Experimental Biology* **144**: 535-549.

Le Corronc H, Alix P and Hue B (2002) Differential sensitivity of two insect GABA-gated chloride channels to dieldrin, fipronil and picrotoxinin. *J Insect Physiol* **48**(4): 419-431.

Lee SJ, Tomizawa M and Casida JE (2003) Nereistoxin and cartap neurotoxicity attributable to direct block of the insect nicotinic receptor/channel. *Journal of Agricultural and Food Chemistry* **51**(9): 2646-2652.

Littleton JT and Ganetzky B (2000) Ion channels and synaptic organization: analysis of the Drosophila genome. *Neuron* **26**(1): 35-43.

Maggio F and King GF (2002a) Role of the structurally disordered N- and C-terminal residues in the janus-faced atracotoxins. *Toxicon* **40**(9): 1355-1366.

Maggio F and King GF (2002b) Scanning mutagenesis of a Janus-faced atracotoxin reveals a bipartite surface patch that is essential for neurotoxic function. *Journal of Biological Chemistry* **277**(25): 22806-22813.

McCaman RE, McKenna DG and Ono JK (1977) A pressure system for intracellular and extracellular ejections of picoliter volumes. *Brain Research* **136**(1): 141-147.

McCutchen BF, Hoover K, Preisler HK, Betana MD, Herrmann R, Robertson JL and Hammock BD (1997) Interactions of recombinant and wild-type baculoviruses with classical insecticides and pyrethroid-resistant tobacco budworm (Lepidoptera: Noctuidae). *Journal of economic entomology* **90**(5): 1170-1180.

Millar N and Denholm I (2007) Nicotinic acetylcholine receptors: targets for commercially important insecticides. *Invertebrate Neuroscience* **7**(1): 53-66.

Millar NS (1999) Heterologous expression of mammalian and insect neuronal nicotinic acetylcholine receptors in cultured cell lines. *Biochem Soc Trans* **27**(6): 944-950.

Millar NS and Lansdell SJ (2010) Characterisation of insect nicotinic acetylcholine receptors by heterologous expression. *Adv Exp Med Biol* **683**: 65-73.

Miller C, Moczydlowski E, Latorre R and Phillips M (1985) Charybdotoxin, a protein inhibitor of single Ca2+-activated K+ channels from mammalian skeletal muscle. *Nature* **313**(6000): 316-318.

Mueller A, Starobova H, Inserra MC, Jin AH, Deuis JR, Dutertre S, Lewis RJ, Alewood PF, Daly NL and Vetter I (2015) alpha-Conotoxin MrIC is a biased agonist at alpha7 nicotinic acetylcholine receptors. *Biochem Pharmacol* **94**(2): 155-163.

Narahashi T, Zhao X, Ikeda T, Salgado VL and Yeh JZ (2010) Glutamate-activated chloride channels: Unique fipronil targets present in insects but not in mammals. *Pestic Biochem Physiol* **97**(2): 149-152.

Orr N, Shaffner AJ, Richey K and Crouse GD (2009) Novel mode of action of spinosad: receptor binding studies demonstrating lack of interaction with known insecticidal target sites.`. *Pesticide Biochemistry and Physiology* **95**: 1-5.

Peng IF and Wu C-F (2007) Differential contributions of Shaker and Shab K^+ currents to neuronal firing patterns in *Drosophila*. *Journal of Neurophysiology* **97**(1): 780-794.

Quick MW and Lester RA (2002) Desensitization of neuronal nicotinic receptors. *J Neurobiol* **53**(4): 457-478.

Salgado VL (1998) Studies on the mode of action of spinosad: insect symptoms and physiological correlates. *Pesticide Biochemistry and Physiology* **60**: 91-102.

Salgado VL and Saar R (2004) Desensitizing and non-desensitizing subtypes of alpha-bungarotoxin-sensitive nicotinic acetylcholine receptors in cockroach neurons. *Journal of insect physiology* **50**(10): 867-879.

Salgado VL and Saar R (2010) The Spinosyns: Chemistry, Biochemistry, Mode of action and Resistance, in *Insect control: Biological and synthetic agents* (Gilbert LI and Gill SS eds) pp 207-243, Academic press, Cambridge, USA.

Salgado VL, Sheets JJ, Watson GB and Schmidt AL (1998) Studies on the mode of action of spinosad: the internal effective concentration and the concentration dependence of neural excitation. *Pesticide Biochemistry and Physiology* **60**: 103-110.

Salgado VL and Sparks TC (2005) 6.5 - The Spinosyns: chemistry, biochemistry, mode of action, and resistance, in *Comprehensive Molecular Insect Science* (Lawrence IG, Kostas I and Sarjeet SG eds) pp 137-173, Elsevier, Amsterdam.

Sanchez M and McManus OB (1996) Paxilline inhibition of the alpha-subunit of the high-conductance calcium-activated potassium channel. *Neuropharmacology* **35**(7): 963-968.

Sanguinetti MC, Johnson JH, Hammerland LG, Kelbaugh PR, Volkmann RA, Saccomano NA and Mueller AL (1997) Heteropodatoxins: peptides isolated from spider venom that block Kv4.2 potassium channels. *Molecular pharmacology* **51**(3): 491-498.

Schulz R, Sawruk E, Mülhardt C, Bertrand S, Baumann A, Phannavong B, Betz H, Bertrand D, Gundelfinger ED and Schmitt B (1998) Dα3, a new functional α subunit of nicotinic acetylcholine receptors from Drosophila. . *J Neurochem* **71**: 853–862.

Simon-Delso N, Amaral-Rogers V, Belzunces LP, Bonmatin JM, Chagnon M, Downs C, Furlan L, Gibbons DW, Giorio C, Girolami V, Goulson D, Kreutzweiser DP, Krupke CH, Liess M, Long E, McField M, Mineau P, Mitchell EA, Morrissey CA, Noome DA, Pisa L, Settele J, Stark JD, Tapparo A, Van Dyck H, Van Praagh J, Van der Sluijs JP, Whitehorn PR and Wiemers M (2015) Systemic insecticides (neonicotinoids and fipronil): trends, uses, mode of action and metabolites. *Environ Sci Pollut Res Int* **22**(1): 5-34.

Stocker M, Stuhmer W, Wittka R, Wang X, Muller R, Ferrus A and Pongs O (1990) Alternative Shaker transcripts express either rapidly inactivating or noninactivating K^+ channels. *PNAS* **87**(22): 8903-8907.

Tedford HW, Maggio F, Reenan RA and King G (2007) A model genetic system for testing the in vivo function of peptide toxins. *Peptides* **28**(1): 51-56.

Thany SH (2009) Agonist actions of clothianidin on synaptic and extrasynaptic nicotinic acetylcholine receptors expressed on cockroach sixth abdominal ganglion. *Neurotoxicology* **30**(6): 1045-1052.

Thany SH (2010) Electrophysiological studies and pharmacological properties of insect native nicotinic acetylcholine receptors. *Adv Exp Med Biol* **683**: 53-63.

Tomizawa M and Casida JE (2003) Selective toxicity of neonicotinoids attributable to specificity of insect and mammalian nicotinic receptors. *Annu Rev Entomol* **48**: 339-364.

Tsunoda S and Salkoff L (1995) Genetic analysis of Drosophila neurons: Shal, Shaw, and Shab encode most embryonic potassium currents. *The Journal of neuroscience : the official journal of the Society for Neuroscience* **15**(3 Pt 1): 1741-1754.

Vetter I and Lewis RJ (2010) Characterisation of endogenous calcium responses in neuronal cell lines. *Biochemical Pharmacology* **79**: 908-920.

Wang J, Kuryatov A, Jin Z, Norleans J, Kamenecka TM, Kenny PJ and Lindstrom J (2015) A Novel alpha2/alpha4 Subtype-selective Positive Allosteric Modulator of Nicotinic Acetylcholine Receptors Acting from the C-tail of an alpha Subunit. *J Biol Chem* **290**(48): 28834-28846.

Wang X-h, Connor M, Smith R, Maciejewski MW, Howden MEH, Nicholson GM, Christie MJ and King GF (2000) Discovery and characterization of a family of insecticidal neurotoxins with a rare vicinal disulfide bridge. *Nature Structural Biology* **7**(6): 505-513.

Watson GB, Chouinard SW, Cook KR, Geng C, Gifford JM, Gustafson GD, Hasler JM, Larrinua IM, Letherer TJ, Mitchell JC, Pak WL, Salgado VL, Sparks TC and Stilwell GE (2010) A spinosyn-sensitive *Drosophila melanogaster* nicotinic acetylcholine receptor identified through chemically induced target site resistance, resistance gene identification, and heterologous expression. *Insect Biochemistry and Molecular Biology* **40**(5): 376-384.

Wei A, Covarrubias M, Butler A, Baker K, Pak M and Salkoff L (1990) K^+ current diversity is produced by an extended gene family conserved in Drosophila and mouse. *Science* **248**(n4955): 599-504.

Wicher D, Walther C and Wicher C (2001) Non-synaptic ion channels in insects -- basic properties of currents and their modulation in neurons and skeletal muscles. *Progress in Neurobiology* **64**(5): 431-525.

Windley MJ, Escoubas P, Valenzuela SM and Nicholson GM (2011) A novel family of insect-selective peptide neurotoxins targeting insect large-conductance calcium-activated K+ channels isolated from the venom of the theraphosid spider *Eucratoscelus constrictus*. *Molecular pharmacology* **80**(1): 1-13.

Windley MJ, Herzig V, Dziemborowicz SA, Hardy MC, King GF and Nicholson GM (2012) Spider-venom peptides as bioinsecticides. *Toxins (Basel)* **4**(3): 191-227.

Yeung SYM, Thompson D, Wang Z, Fedida D and Robertson B (2005) Modulation of K_V3 subfamily potassium currents by the sea anemone toxin BDS: Significance for CNS and biophysical studies. *Journal of Neuroscience* **25**(38): 8735-8745.

Figure Legends

Fig. 1. Effects of paxilline on cockroach DUM neuron $I_{K(V)}$. (A) Representative superimposed current traces showing the typical effect of 10 nM paxilline on $I_{BK(Ca)}$. The peak and late $I_{BK(Ca)}$ are indicated by a circle and square, respectively. (B) Concentration-response curve for κ-HXTX-Hv1c block of $I_{BK(Ca)}$ in DUM neurons. Data was fitted with a Logistic function (see *Materials and Methods*) yielding an IC_{50} of 13.6 ± 1.4 nM and 12.5 ± 1.7 nM (n = 3–9) for block of peak (circles) and late (squares) $I_{BK(Ca)}$, respectively. (C-E) Representative superimposed current traces showing the typical effect of 10 µM paxilline on (C) $I_{K(A)}$, (D) $I_{K(DR)}$, and (E) $I_{K(Na)}$. Grey dotted lines beneath current traces denote zero current. (F) Test pulse protocols used to generate $I_{BK(Ca)}$ (panel A), $I_{K(DR)}$ (panel D) and $I_{K(Na)}$ (panel E). (G) Test pulse protocols used to generate $I_{K(A)}$ (panel C).

Fig. 2. Acute toxicity of $K_{Ca}1.1$, K_A and K_V4 (Shal-like) channel blockers in the house cricket, *Acheta domesticus*. (A) LD_{50} values at 48 h post injection were 167 ± 10 pmol/g and 496 ± 10 nmol/g for κ-HXTX-Hv1c (Wang et al., 2000) and 4-AP, respectively. ChTx, IbTx and paxilline produced no insecticidal activity in house crickets at doses up to 2 nmol/g nor did a combination of κ-SPRTX-Hv1b and IbTx (1:1) injected simultaneously at doses up to 2 nmol/g. (B) Concentration-response curve for lethal (closed circles) and knockdown (closed squares) effects of 4-AP. Data were fitted with Eq. 2 generating LD_{50} and KD_{50} values of 496 ± 10 and 410 ± 7 nmol/g, respectively. All acute toxicity data represents the mean lethality and knockdown values ± SE recorded at 48 h post-injection from at least three independent trials. (C-E) Typical spontaneous overshooting action potentials recorded in DUM neurons before (black traces), and following a 5-min perfusion with (C) 100 nM κ-HXTX-Hv1c (cyan trace), (D) 100 nM IbTx (green trace), and (E) 5 mM 4-AP (blue trace). (F) Mean spontaneous action potential firing frequency in the presence of 3 and 100 nM κ-HXTX-Hv1c (cyan), 100 nM IbTx (green) and 5 mM 4-AP (blue). $*p < 0.05$, one-way ANOVA.

Fig. 3. Effects of κ-HXTX-Hv1c on cockroach DUM neuron $I_{K(A)}$. (A) Typical effect of a saturating concentration of κ-HXTX-Hv1c on $I_{K(A)}$. Currents were recorded by offline subtraction of the currents generated by the two-pulse protocol with test pulse +40 mV shown in panel D. (B) Concentration-response curve for κ-HXTX-Hv1c block of peak $I_{K(A)}$ in DUM neurons (n = 3–5). Data was fitted with a Logistic function (see *Materials and Methods*) yielding an IC_{50} of 85 ± 39 nM and a maximal inhibition of 36.1 ± 4.2% of $I_{K(A)}$. (C) $I_{K(A)}$-V relationship for the block by 1 µM κ-HXTX-Hv1c. Currents were recorded by offline subtraction of the currents generated by the two-pulse protocol with test pulses from –80 to +60 mV in 10-mV steps shown in panel D. Grey dotted lines beneath current traces in panels A-C denote zero current.

Fig. 4. Effects of K_V channel modulators on cockroach DUM neuron $I_{K(A)}$ and $I_{K(DR)}$. (A, C) Superimposed $I_{K(A)}$ traces illustrating the typical effects of (A) 200 nM κ-TRTX-Ps1a (red), (C) 1 μM margatoxin (red). (B) Representative trace showing the typical effect of 1 μM BDS-I on $I_{K(DR)}$ (red). Currents were recorded in response to the test pulse protocol shown in panel H. (D) Representative trace of $I_{K(A)}$ illustrating the lack of further inhibition by 500 nM κ-SPRTX-Hv1b following prior inhibition by 500 nM κ-HXTX-Hv1c. Traces were generated by offline subtraction of the currents evoked by the test pulse protocol shown in panel G. (E, F) Complementary experiments to show lack of additional block of $I_{K(A)}$ by κ-SPRTX-Hv1b (pink) or κ-HXTX-Hv1c (cyan) following inhibition by κ-HXTX-Hv1c or κ-SPRTX-Hv1b, respectively (n = 3–5).

Fig. 5. Minor effects of K_V channel modulators on cockroach DUM neuron $I_{K(Na)}$. (A) Representative superimposed current traces illustrating the isolation of $I_{K(Na)}$ using 300 nM TTX. The sodium-sensitive portion of the current, generated using the pulse protocol in panel C, is blocked by TTX (grey shaded trace). The remaining current was digitally subtracted offline to isolate $I_{K(Na)}$ shown in panel B that demonstrates the modest effect of 1 μM κ-HXTX-Hv1c (cyan).

Fig. 6 Concentration-dependent effects of κ-HXTX-Hv1c on nAChR-mediated currents in cockroach DUM neurons. (A) Inward I_{nAChR} were evoked in response to 10-ms pulse applications of 10 μM nicotine. Traces show the typical effects of increasing concentrations of κ-HXTX-Hv1c on I_{AChR}. (B-C) Traces from A were overlaid and the current magnified to highlight the lack of effect of increasing concentrations of κ-HXTX-Hv1c on (B) peak I_{nAChR} amplitude and (C) the slowed rate of I_{nAChR} decay in the presence of toxin. t_{20}: duration of I_{nAChR} at 20% of maximum current amplitude. (D) Effect of 500 nM α-BgTx on inward I_{nAChR} evoked in response to 10-ms pulse applications of 10 μM nicotine. (E) Lack of activation of any current by direct application of 1 μM κ-HXTX-Hv1c. The dotted gray line in panels A-D represents zero current.

Fig. 7. Effect of κ-HXTX-Hv1c on I_{nAChR} amplitude and decay. (A) Comparison of peak I_{nAChR} amplitude values in the presence of increasing concentrations of κ-HXTX-Hv1c or 500 nM α-bungarotoxin (α-BgTx) (n = 3–8). (B) Concentration-response curve for I_{nAChR} duration$_{20}$ in the presence of increasing concentrations of κ-HXTX-Hv1c. Data were fitted with a Logistic function (see *Materials and Methods*) yielding an EC_{50} value of 180 ± 30.4 nM (n = 3–4). (C) Concentration-response curve for control (black circles) and 200 nM κ-HXTX-Hv1c (cyan circles) I_{nAChR} t_{20} in response to increasing durations of 10 μM nicotine application, yielding EC_{50} values of 8.5 ± 0.5 ms and 6.6 ± 0.5 ms (n = 3–4), respectively. Data were normalized to the maximal control nicotine response. *p < 0.05, **p < 0.01, ***p < 0.001, one-way ANOVA. (D) I_{nAChR}-V relationship in the

absence (black circles), and presence (cyan circles), of 200 nM κ-HXTX-Hv1c (n = 3). Currents were generated by the test pulse protocol in the inset of panel D. Arrowheads denote timing of the application of a 10 ms pulse of nicotine. Data were normalized to the maximal nicotine response.

Fig. 8. Effects of κ-HXTX-Hv1c on partially and fully desensitized nAChR channels in cockroach DUM neurons. I_{nAChR} were recorded in response to 3.5–5 min continuous applications of 10 µM nicotine in the absence (A), and in the presence of 200 nM (B) and 500 nM (C, D) κ-HXTX-Hv1c. Toxin was applied 100 s into nicotine perfusion, following partial (B, C) or full (D) desensitization of I_{nAChR}.

Fig. 9. Minor effects of κ-HXTX-Hv1c on I_{GluClR} in cockroach DUM neurons. (A-B) Superimposed traces showing typical effects of (A) 1 µM κ-HXTX-Hv1c and (B) 100 µM picrotoxin on $I_{Glu\text{-}Cl}$. (C) Comparison of $I_{Glu\text{-}Cl}$ amplitude in response to increasing concentrations of κ-HXTX-Hv1c (n = 3–4) and 100 µM picrotoxin (PTX; n = 3). (D) Lack of effect of κ-HXTX-Hv1c on $I_{Glu\text{-}Cl}$ duration. t_{20}: $I_{Glu\text{-}Cl}$ duration at 20% of control current amplitude. $^{**}p < 0.01$, $^{****}p < 0.0001$, one-way ANOVA. (E) Families of superimposed currents generated by 2.5–1520 ms pulses of 100 µM glutamate in the absence (Ea), and presence (Eb), of 1 µM κ-HXTX-Hv1c. (F) Concentration-response curve of $I_{Glu\text{-}Cl}$ amplitude in response to the application of 100 µM glutamate for varying durations in the absence (closed circles), and presence (red circles), of 1 µM κ-HXTX-Hv1c, yielding EC_{50} values of 17.8 ± 1.4 ms and 12.6 ± 3.4 ms (n = 3–5), respectively. Data were normalized to the maximal control $I_{Glu\text{-}Cl}$ amplitude in response to 100 µM glutamate.

Fig. 10. Lack of effect of κ-HXTX-Hv1c on I_{GABAR} in cockroach DUM neurons. (A-B) Superimposed traces showing typical effects of (A) 1 µM κ-HXTX-Hv1c and (B) 100 µM picrotoxin on $I_{GABA\text{-}Cl}$. (C) Comparison of $I_{GABA\text{-}Cl}$ amplitude in the presence of κ-HXTX-Hv1c and picrotoxin (n = 4–5). (D) Lack of effect of κ-HXTX-Hv1c on $I_{GABA\text{-}Cl}$ duration (n = 3–4). t_{20}: I_{GABAR} duration at 20% of maximum current amplitude. $^{****}p < 0.0001$, one-way ANOVA.

Fig. 11. Lack of affinity of κ-HXTX-Hv1c for vertebrate α7 and α3*nAChRs. Concentration–response relationships for inhibition of neuronal α7 and ganglionic-type α3* nAChR responses in SH-SY5Y neuroblastoma cells. Data was fitted with a Logistic function (see *Materials and Methods*). Lack of effect of κ-HXTX-Hv1c (cyan symbols, dashed lines) on vertebrate α7 (A) and α3* (B) nAChR responses. *d*-Tubocurarine (black symbols, solid lines) was included as a positive control in both assays. Data represent the mean ± SEM of n = 3 experiments. (C) Enhancement of the response of α3* nAChRs to nicotine (beige circles) by the addition of the type II PAM, PNU120596 (red circles). Nicotine was applied at time zero. Data represent the mean ± SEM (n = 4).

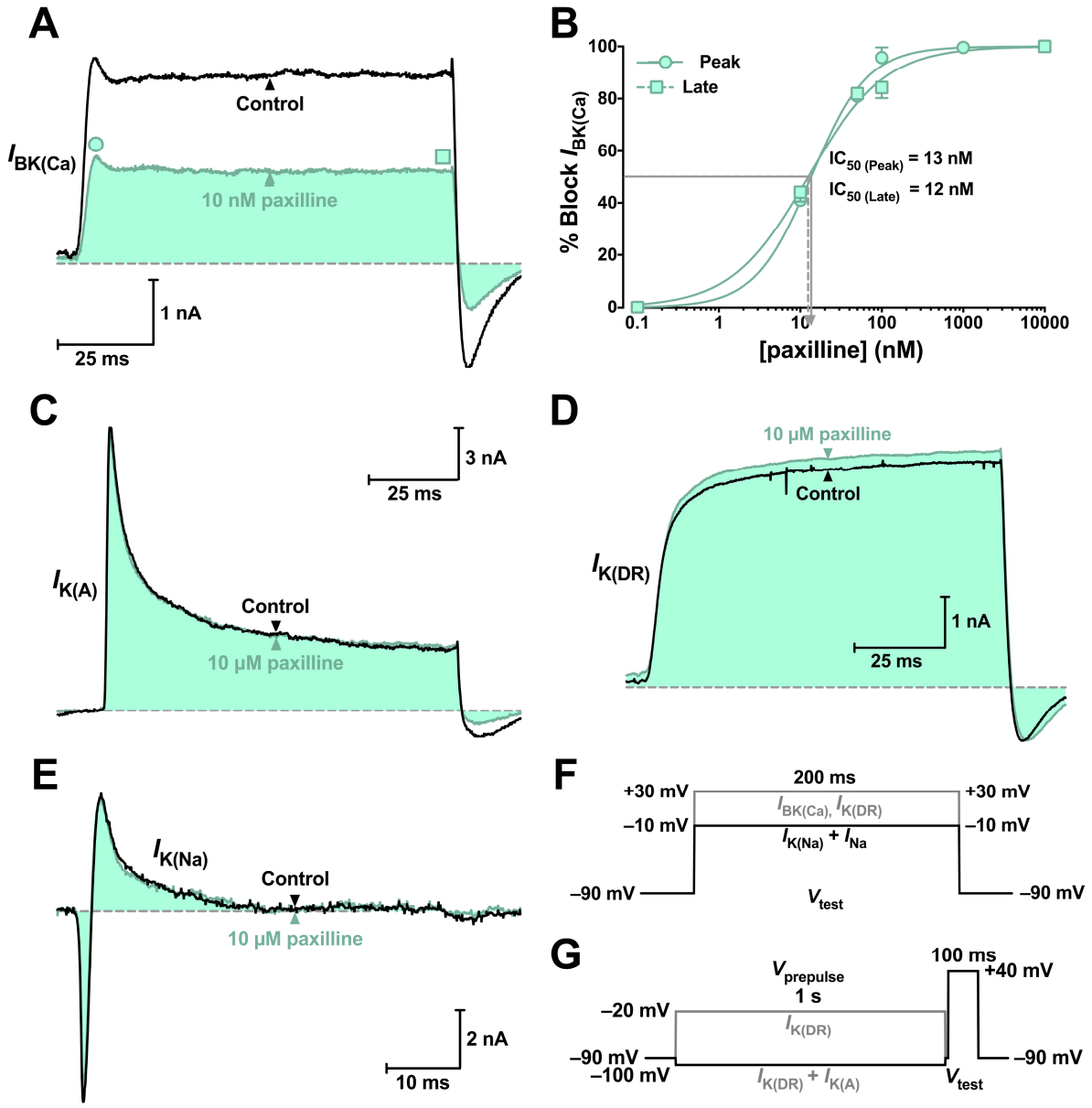
A
Control
$I_{BK(Ca)}$
10 nM paxilline
1 nA
25 ms
B
Peak
Late
% Block $I_{BK(Ca)}$
$IC_{50\ (Peak)}$ = 13 nM
$IC_{50\ (Late)}$ = 12 nM
[paxilline] (nM)
C
3 nA
25 ms
$I_{K(A)}$
Control
10 µM paxilline
D
10 µM paxilline
Control
$I_{K(DR)}$
1 nA
25 ms
E
$I_{K(Na)}$
Control
10 µM paxilline
2 nA
10 ms
F
200 ms
+30 mV
–10 mV
–90 mV
$I_{BK(Ca)}$, $I_{K(DR)}$
$I_{K(Na)}$ + I_{Na}
V_{test}
G
100 ms
$V_{prepulse}$
1 s
–20 mV
–90 mV
–100 mV
+40 mV
$I_{K(DR)}$
$I_{K(DR)}$ + $I_{K(A)}$
V_{test}

Figure 1

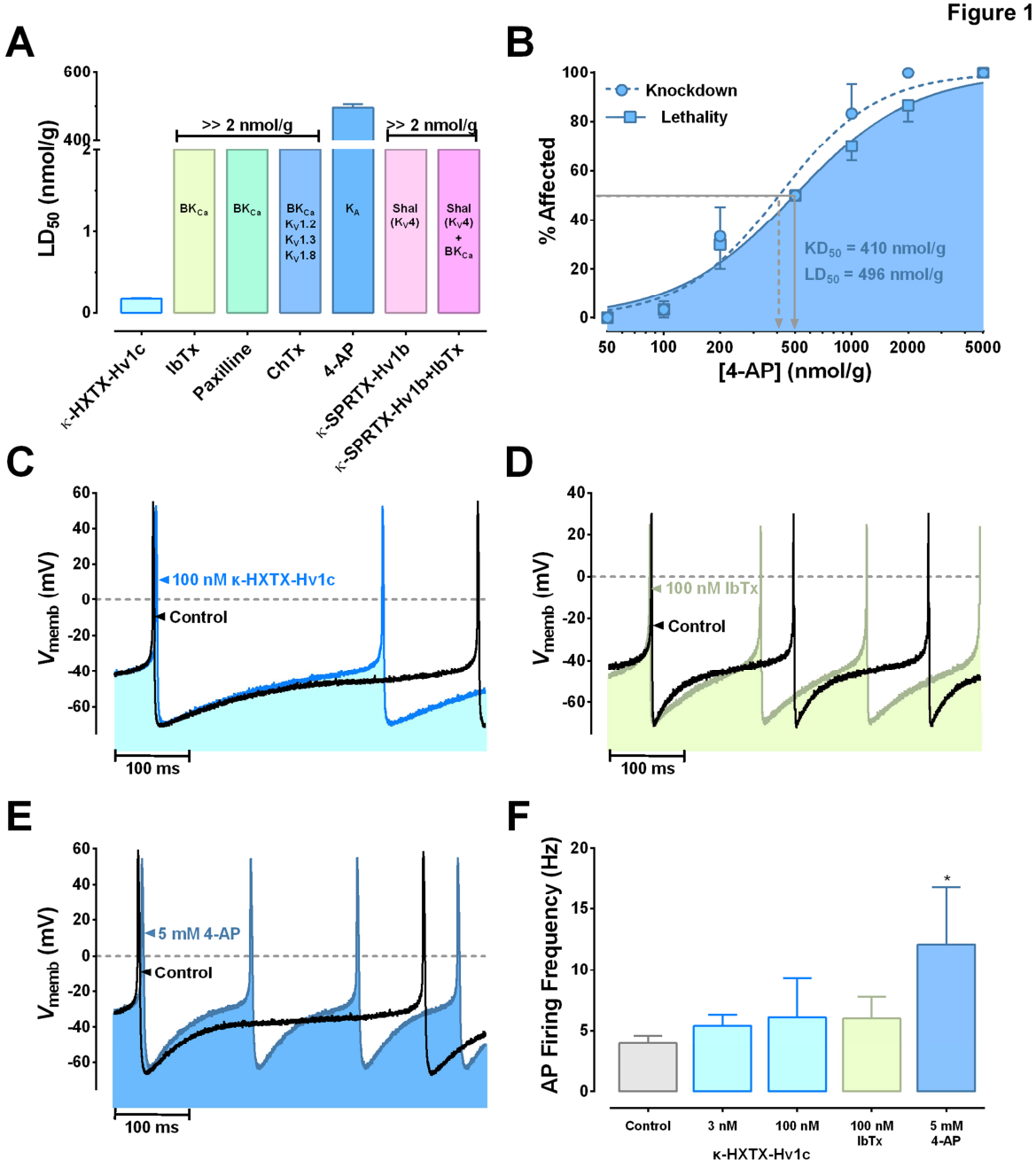
A
LD50 (nmol/g)
>> 2 nmol/g
>> 2 nmol/g
BKCa
BKCa
BKCa KV1.2 KV1.3 KV1.8
KA
Shal (KV4)
Shal (KV4) + BKCa
κ-HXTX-Hv1c
IbTx
Paxilline
ChTx
4-AP
κ-SPRTX-Hv1b
κ-SPRTX-Hv1b+IbTx
B
Knockdown
Lethality
% Affected
KD50 = 410 nmol/g
LD50 = 496 nmol/g
[4-AP] (nmol/g)
C
Vmemb (mV)
100 nM κ-HXTX-Hv1c
Control
100 ms
D
Vmemb (mV)
100 nM IbTx
Control
100 ms
E
Vmemb (mV)
5 mM 4-AP
Control
100 ms
F
AP Firing Frequency (Hz)
Control
3 nM
100 nM
100 nM IbTx
5 mM 4-AP
κ-HXTX-Hv1c

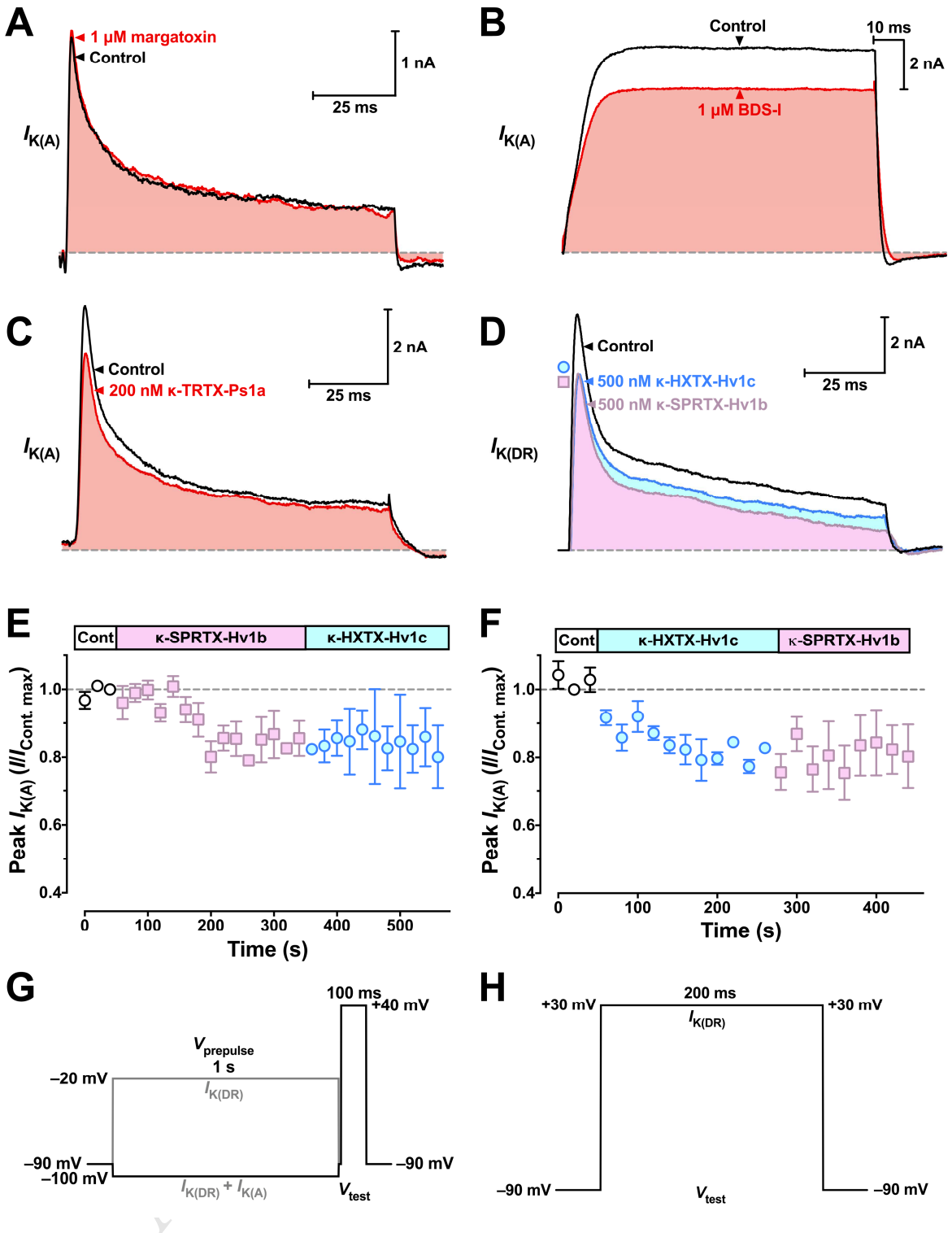
A
1 μM margatoxin
Control
1 nA
25 ms
$I_{K(A)}$
B
Control
10 ms
2 nA
1 μM BDS-I
$I_{K(A)}$
C
Control
200 nM κ-TRTX-Ps1a
2 nA
25 ms
$I_{K(A)}$
D
Control
500 nM κ-HXTX-Hv1c
500 nM κ-SPRTX-Hv1b
2 nA
25 ms
$I_{K(DR)}$
E
Cont
κ-SPRTX-Hv1b
κ-HXTX-Hv1c
Peak $I_{K(A)}$ ($I/I_{Cont.\ max}$)
1.0
0.8
0.6
0.4
0
100
200
300
400
500
Time (s)
F
Cont
κ-HXTX-Hv1c
κ-SPRTX-Hv1b
Peak $I_{K(A)}$ ($I/I_{Cont.\ max}$)
1.0
0.8
0.6
0.4
0
100
200
300
400
Time (s)
G
100 ms
+40 mV
$V_{prepulse}$
1 s
–20 mV
$I_{K(DR)}$
–90 mV
–100 mV
–90 mV
$I_{K(DR)}$ + $I_{K(A)}$
V_{test}
H
+30 mV
200 ms
$I_{K(DR)}$
+30 mV
–90 mV
V_{test}
–90 mV

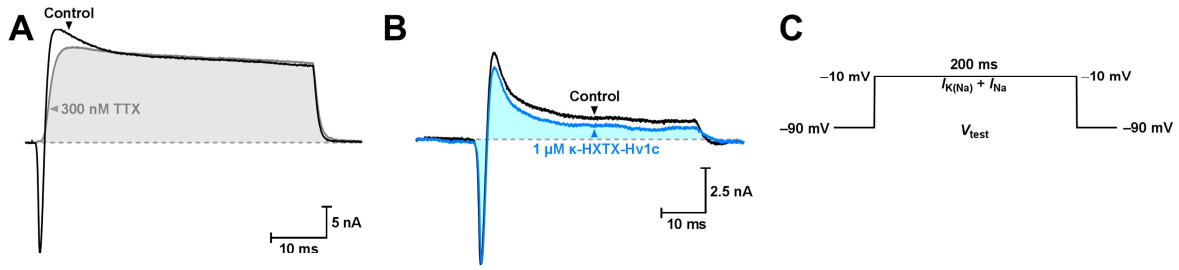

Figure 5

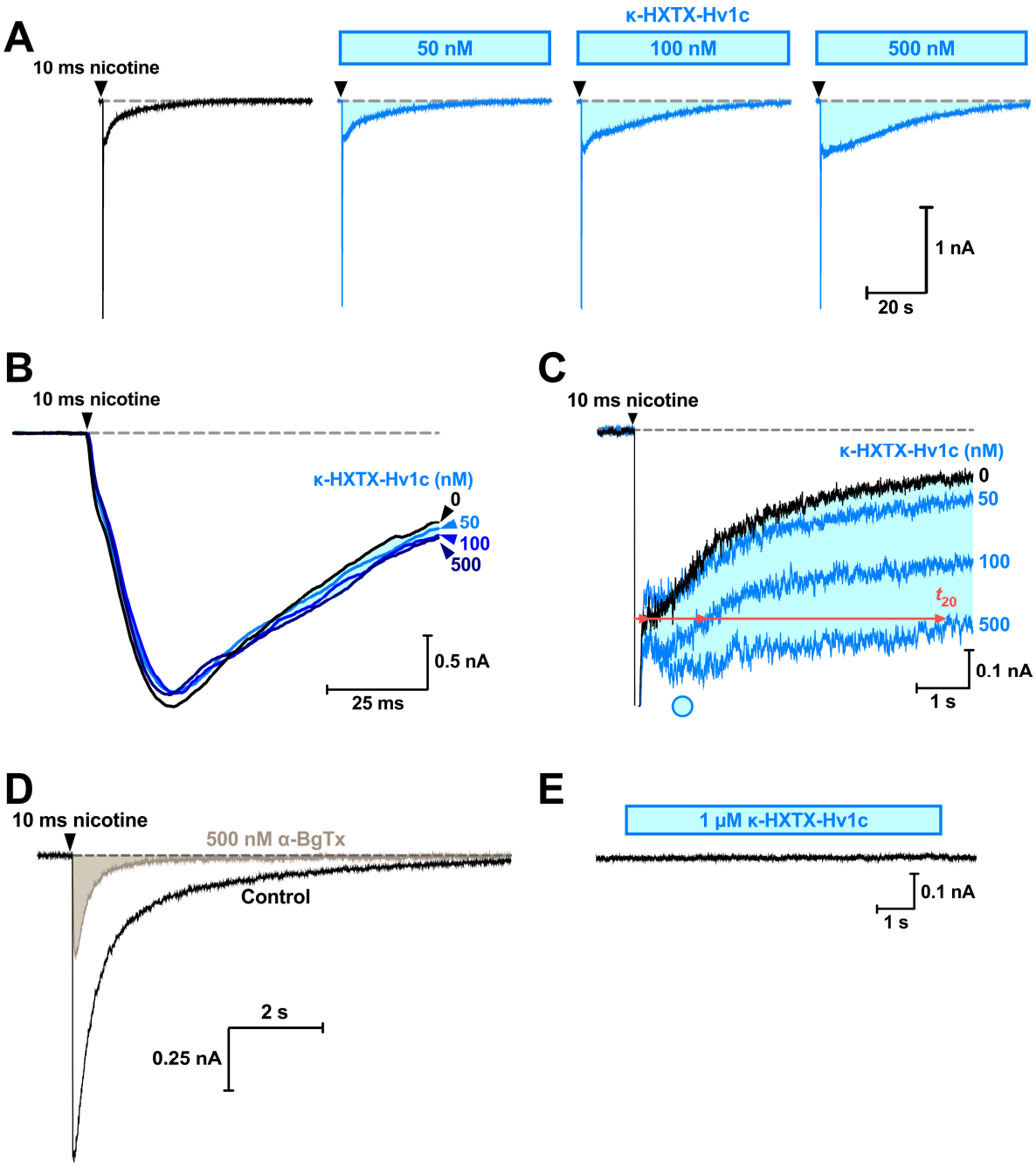
A
10 ms nicotine
κ-HXTX-Hv1c
50 nM
100 nM
500 nM
1 nA
20 s
B
10 ms nicotine
κ-HXTX-Hv1c (nM)
0
50
100
500
0.5 nA
25 ms
C
10 ms nicotine
κ-HXTX-Hv1c (nM)
0
50
100
500
t_{20}
0.1 nA
1 s
D
10 ms nicotine
500 nM α-BgTx
Control
2 s
0.25 nA
E
1 μM κ-HXTX-Hv1c
0.1 nA
1 s

Figure 6

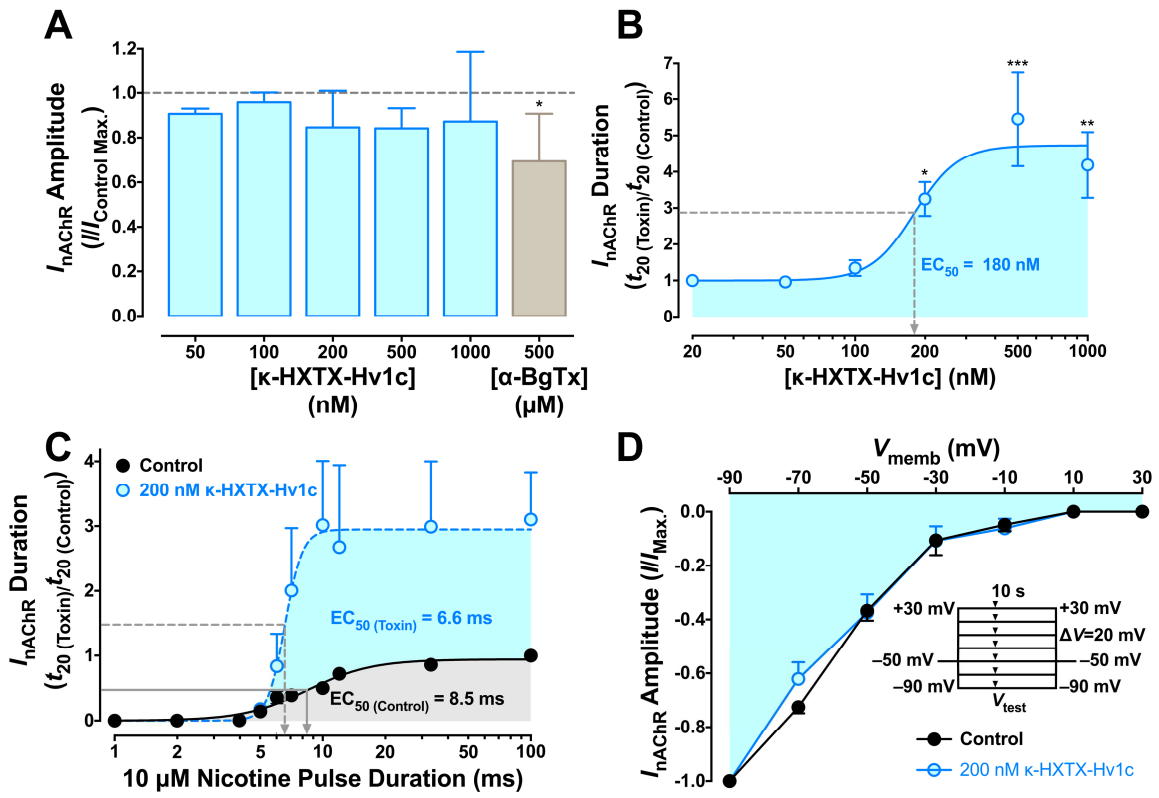

Figure 7

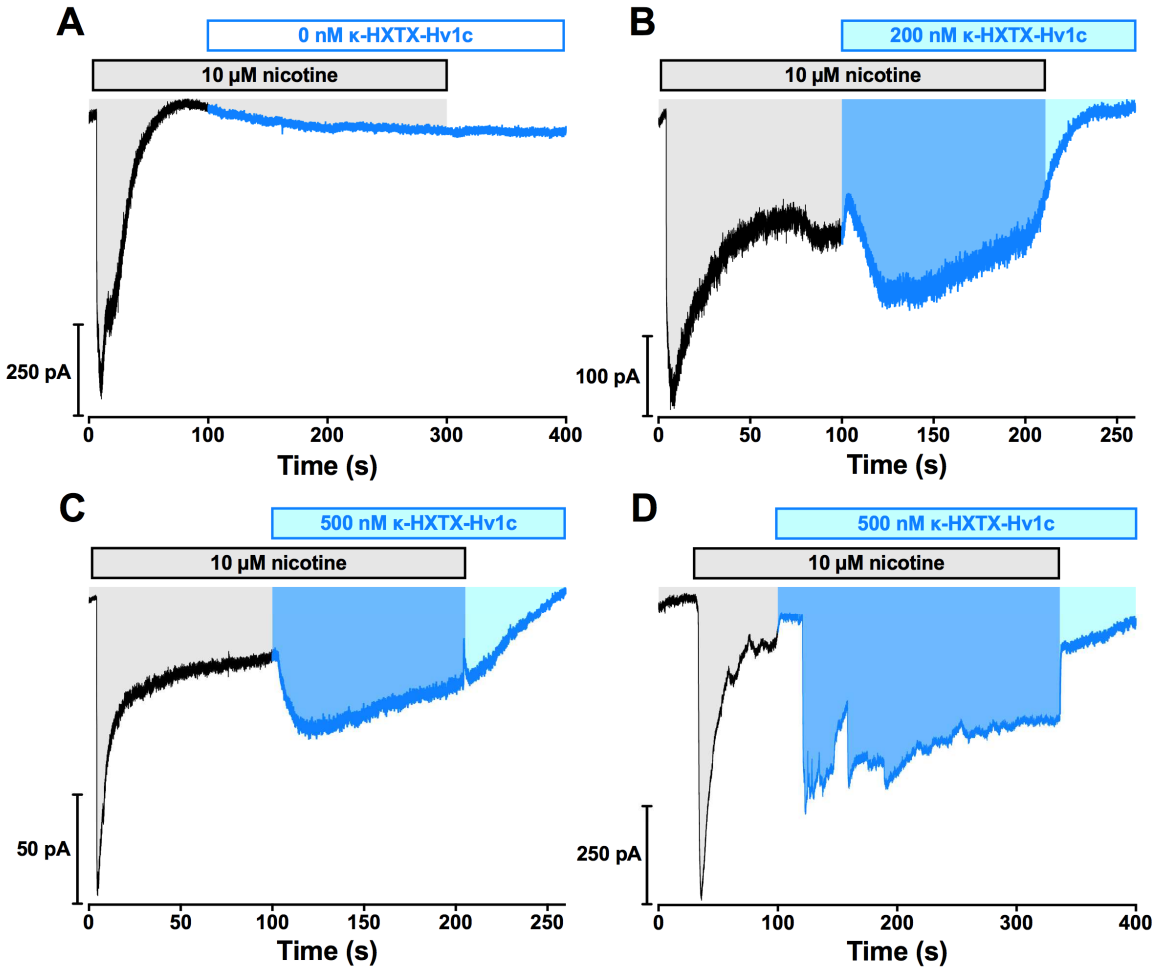

Figure 8

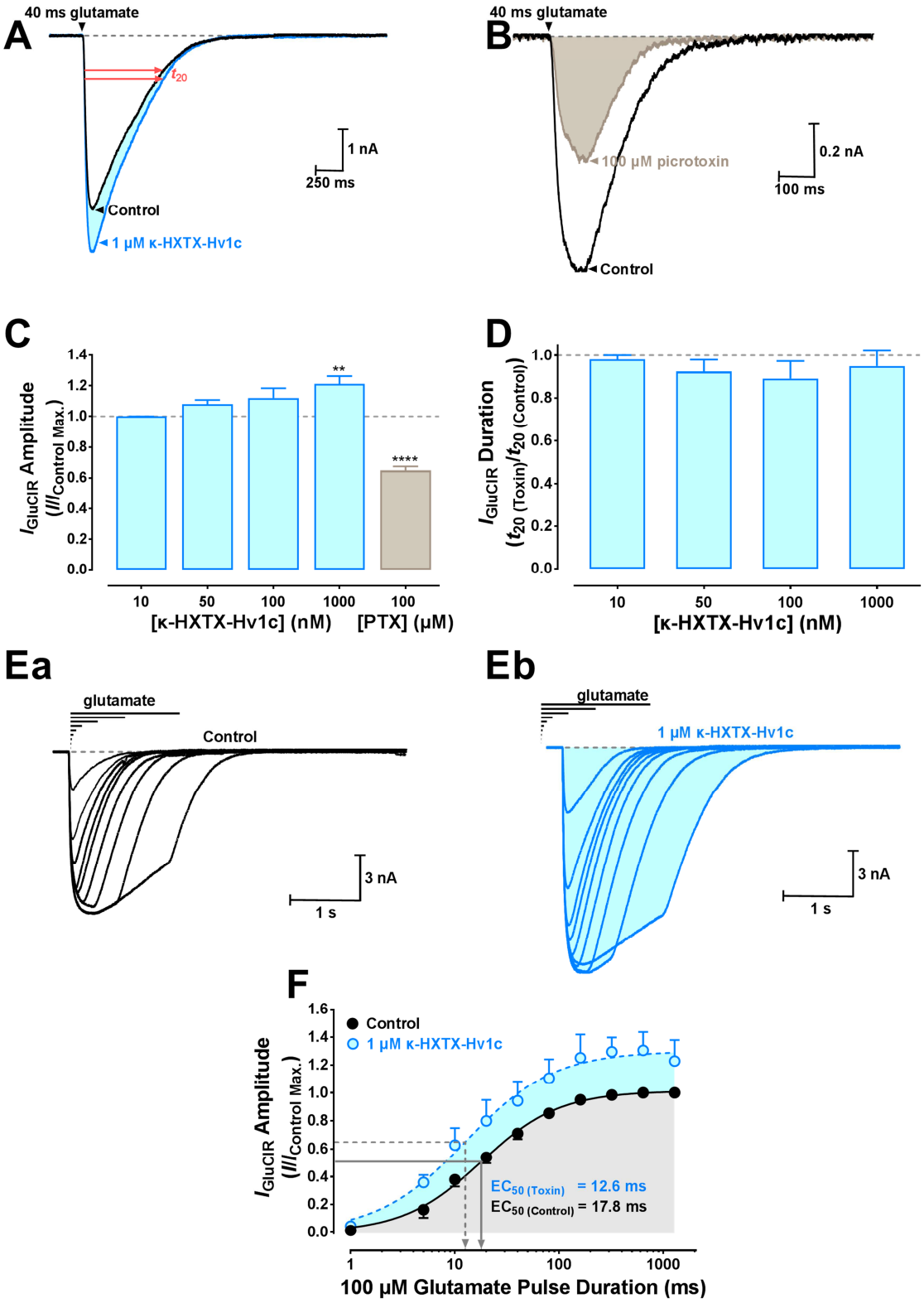
A
40 ms glutamate
t_{20}
1 nA
250 ms
Control
1 μM κ-HXTX-Hv1c
B
40 ms glutamate
100 μM picrotoxin
0.2 nA
100 ms
Control
C
I_{GluCIR} Amplitude (I/I Control Max.)
**
****
10
50
100
1000
100
[κ-HXTX-Hv1c] (nM)
[PTX] (μM)
D
I_{GluCIR} Duration (t_{20} (Toxin)/t_{20} (Control))
10
50
100
1000
[κ-HXTX-Hv1c] (nM)
Ea
glutamate
Control
3 nA
1 s
Eb
glutamate
1 μM κ-HXTX-Hv1c
3 nA
1 s
F
Control
1 μM κ-HXTX-Hv1c
I_{GluCIR} Amplitude (I/I Control Max.)
$EC_{50\ (Toxin)}$ = 12.6 ms
$EC_{50\ (Control)}$ = 17.8 ms
100 μM Glutamate Pulse Duration (ms)

Figure 9

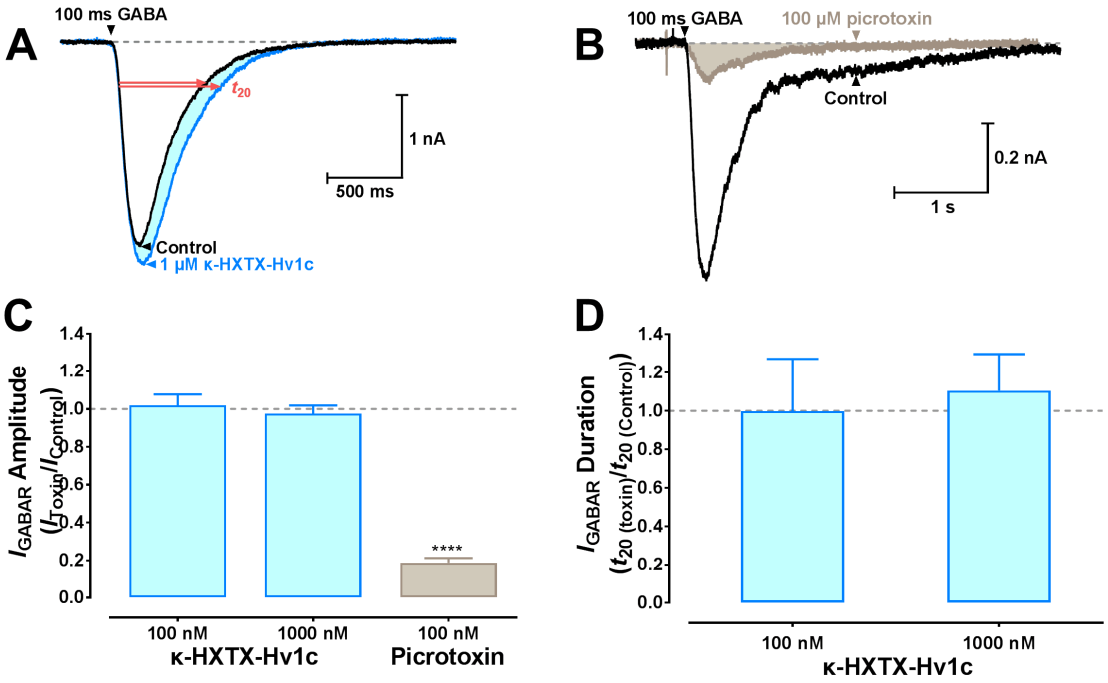

Figure 10